NASA TECHNICAL MEMORANDUM

NASA TM X-64925

ATMOSPHERIC DIFFUSION PREDICTIONS FOR THE EXHAUST EFFLUENTS FROM THE LAUNCH OF A TITAN IIIC, DECEMBER 13, 1973

J. Briscoe Stephens, Editor
Space Sciences Laboratory

September 27, 1974

NASA

George C. Marshall Space Flight Center
Marshall Space Flight Center, Alabama

MSFC - Form 3190 (Rev June 1971)

TECHNICAL REPORT STANDARD TITLE PAGE

1. REPORT NO.	2. GOVERNMENT ACCESSION NO.	3. RECIPIENT'S CATALOG NO.
NASA TM X-64925		

4. TITLE AND SUBTITLE	5. REPORT DATE
Atmospheric Diffusion Predictions for the Exhaust Effluents from the Launch of a Titan IIIC, December 13, 1973	September 27, 1974
	6. PERFORMING ORGANIZATION CODE
7. AUTHOR(S) J. Briscoe Stephens, Editor	8. PERFORMING ORGANIZATION REPORT #
9. PERFORMING ORGANIZATION NAME AND ADDRESS George C. Marshall Space Flight Center Marshall Space Flight Center, Alabama 35812	10. WORK UNIT NO.
	11. CONTRACT OR GRANT NO.
12. SPONSORING AGENCY NAME AND ADDRESS National Aeronautics and Space Administration Washington, D.C. 20546	13. TYPE OF REPORT & PERIOD COVERED Technical Memorandum
	14. SPONSORING AGENCY CODE

15. SUPPLEMENTARY NOTES

Prepared by Space Sciences Laboratory, Science and Engineering

16. ABSTRACT

Results for the predictions with the NASA/MSFC Multilayer Diffusion Model for the dispersive transport of the Titan IIIC rocket exhaust effluents for the 1857 EST launch on December 13, 1973, from the Eastern Test Range at Cape Canaveral Air Force Station are presented. This atmospheric assessment was made in support of the joint Marshall Space Flight Center, Langley Research Center, and Kennedy Space Center rocket exhaust prediction and measurement program. These predictions were primarily intended to define a monitoring grid and for a postflight assessment of the field measurements in order to improve diffusion prediction techniques.

17. KEY WORDS	18. DISTRIBUTION STATEMENT
Fluid Mechanics Aerospace Rocket Effluent Dispersion Modeling Atmospheric	Unclassified - Unlimited J. Briscoe Stephens

19. SECURITY CLASSIF. (of this report)	20. SECURITY CLASSIF. (of this page)	21. NO. OF PAGES	22. PRICE
Unclassified	Unclassified	81	NTIS

MSFC - Form 3292 (Rev December 1972)

For sale by National Technical Information Service, Springfield, Virginia 22151

ACKNOWLEDGMENT

This document presents work done by personnel on the Atmospheric Diffusion/Environmental Assessment Technical Team of the Atmospheric Dynamics Branch (ES43), Aerospace Environment Division, Space Sciences Laboratory, Marshall Space Flight Center, Alabama. Mr. R. K. Dumbauld and Mr. Jay R. Bjorklund of the H. E. Cramer Company, Salt Lake City, Utah, made significant contributions to this overall effort. The comments made by Dr. Roger Stewart, Langley Research Center, were both enlightening and helpful.

TABLE OF CONTENTS

TABLE OF CONTENTS (Concluded)

LIST OF ILLUSTRATIONS

LIST OF TABLES

SYMBOLS AND DEFINITIONS

Equations

$D(x, y, z)$	= dosage at the point x, y, and z (ppm-sec or mg sec/m^3)
F	= bouyancy term in the instantaneous cloud rise formula $= \dfrac{3gQ_H}{4c_p \pi T_s \rho_s}$
H	= height of the stabilized exhaust cloud (m)
$K(r, t, p, T)$	= diffusion coefficient
L_i	= ith dimension of the rocket exhaust cloud (m)
M	= molecular weight (g/mole)
Q_H	= heat release source strength (cal)
Q_M	= mass source strength of the exhaust cloud (ppm)
R	= universal gas constant (0.289 Joule/g °K)
T	= temperature (°K)
c_p	= specific heat of air at constant pressure (0.24 cal/g °K or 1.003 Joules/g °K)
f	= fractional amount of the total effluent which is released by the rocket in the surface mixing layer
g	= gravitational acceleration (9.8 m/sec^2)
m	= power law exponent for the vertical profile of the wind azimuth
p	= power law exponent for the wind speed
q	= power law exponent for the vertical profile of the standard deviation of wind elevation angle in the surface mixing layer

SYMBOLS AND DEFINITIONS (Continued)

r_R = initial cloud radius at the rocket exit (m)

s = stability parameter

$= \frac{g}{T} \frac{\partial \Phi}{\partial z}$ (sec^{-2})

t = time required for the exhaust cloud to reach equilibrium with the atmosphere at the stabilization height (sec)

$\bar{u}$ = mean (time) wind speed (m/sec)

$\langle u \rangle$ = average (space) wind speed (m/sec)

x = downrange distance in the wind direction from the point of cloud stabilization (m)

y = distance from the centerline along the wind direction (m)

z = height of the stabilized exhaust cloud (m)

α = horizontal diffusion coefficient (α = 1)

β = vertical diffusion coefficient (β = 1)

γ = entrainment coefficient (Titan: 0.64)

ρ = density of the ambient air (mg/m^3)

σ_i = standard deviation of the distribution of the exhaust effluents in the exhaust cloud in the ith direction (m)

$= \frac{L_i}{4.3}$ (m)

σ_{AR} = standard deviation of the wind azimuth angle at the surface (deg)

σ_{AT} = standard deviation of the wind azimuth angle at the top of the layer (deg)

SYMBOLS AND DEFINITIONS (Continued)

σ_{ER}	= standard deviation of the wind elevation at the surface (deg)
σ_{ET}	= standard deviation of the wind elevation angle at the top of the surface mixing layer (deg)
Φ	= potential temperature (°K)
$\frac{\partial \Phi}{\partial z}$	= vertical gradient of the potential temperature (Φ)
$\Delta\Theta$	= change in wind direction between the top and bottom of the surface mixing layer
	= $\Theta_T - \Theta_B$ (deg)
$\chi(\vec{r}, t)$	= the concentration (ppm or mg/m^3)

Terms

Centerline: the radial vector in the direction of the mean wind direction whose origin is the point of cloud stabilization.

Concentration: the amount of th effluent present at a specific time. The average concentration is the average amount present during the event.

Dosage: the measure of the total amount of effluent (time integrated concentration) due to the launch vehicle at a specific location.

Ground Cloud: that cloud of rocket effluents emitted during the initial phase of vehicle launch. This cloud is assumed to have an ellipsoidal shape.

Plume Cloud: the cloud of rocket effluents emitted from the vehicle in flight. This cloud has a cylindrical shape whose height is defined by the vertical thickness of the layer.

SYMBOLS AND DEFINITIONS (Concluded)

Potential Temperature (Φ):	the temperature a volume of dry air would have if brought adiabatically from its initial state to the standard press[illegible] of 100 mb.
Quasiadiabatic Layer:	a layer in which the vertical potential temperature gradient is zero or less.
Stable Layer:	a layer in which the vertical potential temperature gradient is positive.

TECHNICAL MEMORANDUM X-64925

ATMOSPHERIC DIFFUSION PREDICTIONS FOR THE EXHAUST EFFLUENTS FROM THE LAUNCH OF A TITAN IIIC, DECEMBER 13, 1973

SUMMARY

J. Briscoe Stephens, Editor

Forecasts and predictions for the dispersive transport of the Titan IIIC rocket exhaust effluents launch at 1857 EST on December 13, 1973, from the Eastern Test Range were obtained utilizing the NASA/MSFC Multilayer Diffusion Model. These forecasts and predictions were employed by personnel of Langley Research Center to determine the deployment of their rocket exhaust effluent monitoring grid.

In the past, the calculations for these predictions were performed on computers located at Marshall Space Flight Center and the results were transmitted to the launch site. Real-time diffusion calculations were performed for the first time onsite at the Range Control Center, Cape Canaveral Air Force Station, on a programmable desk calculator — the MSFC computer computations were used only as backup computations. The results showed that in spite of certain limitations, onsite real-time calculations were superior to the remot calculations because the graphics were feasible with onsite predictions. The data reduction time for the online calculations was approximately 30 minutes.

Our diffusion predictions for this launch showed that the surface maximum concentration for this Titan III exhaust ground cloud did not exceed the environment standards. The exhaust cloud was transported out to sea.

This launch clearly taught us that the land-sea interface must be taken into account in the exhaust cloud height predictions — especially at night when large temperature gradients exist. We can further conclude from a postflight analysis that our predicted concentration fields were stronger than actually measured. This was due, in part, to a lower altitude prediction for the ground cloud stabilization.

SECTION I. INTRODUCTION

J. Briscoe Stephens and Leonard L. DeVries

The NASA/MSFC Multilayer Diffusion Model has been utilized to predict the dispersion of the effluents from the Titan IIIC vehicle which was launched from the Eastern Test Range at Cape Canaveral Air Force Station at 1857 EST on December 13, 1973, (Launch Number 7433). These predictions were made in real time at the Range Control Center on a desk calculator [1], backed up by computer predictions [2] at Marshall Space Flight Center.

The National Environmental Policy Act of 1969 and the April 23, 1972, guidelines of the Council on Environmental Quality require impact statements for assessing the environmental perturbations from the Space Shuttle and other NASA space vehicle rocket motor effluents. Development of quantitative procedures for estimating the space vehicle rocket motor exhaust effluents hazard has been underway for over a decade at the NASA's Marshall Space Flight Center. These computerized procedures for estimating the tropospheric transport of potentially toxic exhaust effluents have been developed [1, 2] based on Gaussian diffusion modeling techniques. In addition to estimates of atmospheric transport, estimates of dispersion and decay of all airborne toxic material released as a result of normal launch operations must also be provided for cases involving fuel spillage, vehicle abort, or vehicle destruct situations.

Universally accepted and adequately validated prediction techniques for the rocket motor effluent problem are not available, and much uncertainty exists concerning very important aspects of the problem, such as: the amount and composition of the rocket engine effluents and their dispersal and transport in the atmosphere. The available atmospheric measurements to ascertain the reliability of the description of rocket effluent dispersion models in the atmosphere are sparse and still of questionable accuracy. On the other hand, the requirements for estimating toxic fuel hazards clearly exist in order to establish special constraints on operations, test, and launch activities to assure that allowable concentrations of these effluents will not be exceeded. The need for implementing a program for monitoring rocket engine exhaust effluents has been recognized for many years. As a result of informal discussions between representatives of NASA Headquarters, Marshall Space Flight Center, Langley Research Center, and Kennedy Space Center, it became apparent that a NASA in-house rocket engine effluent prediction and measurement program was desirable, possible, and feasible; therefore, such a program was initiated in 1972.

A joint solid rocket motor exhaust prediction (Marshall) and measurement (Langley supported by Kennedy) program has evolved utilizing the Titan launches as a source for empirical information that can be employed to more accurately predict the environmental impact of the Space Shuttle under varying atmospheric conditions. Determination of the locations for the sensor matrix and the sampling interval at each location, which is dependent on the atmospheric thermodynamics and kinematics, affords an operational capability for a real-time forecast for the transport and dispersion of these exhaust effluents. This forecast is performed with the NASA/MSFC Multilayer Diffusion Model. Since a real-time requirement exists it was considered more efficient to reduce the generality of the NASA/MSFC Multilayer Diffusion Algorithms to a degree where the primary calculations could be done on a programmable desk calculator (HP 9820) at Cape Canaveral and backup calculations of greater detail could be performed at Marshall Space Flight Center on computers.

Before considering the results of the predictions for the dispersive transport of the Titan exhaust effluents from this launch, a brief summary of the NASA/MSFC Multilayer Diffusion Modeling techniques is given. The detailed discussion of the models and algorithms associated with this modeling are given in the appendices.

SECTION II. NASA/MSFC MULTILAYER DIFFUSION MODEL

J. Briscoe Stephens

The spatial description, in terms of concentration and dosage, of the dispersive transport of effluents from a discrete source is afforded by the NASA/MSFC Multilayer Diffusion Model. Specifically, this application of the model is for the prediction of the concentration distribution associated with the rocket exhaust effluents emitted during the launch of a Titan III vehicle in order to ascertain the grid for the effluent monitoring matrix and the operation interval for the sensors. This application also permits the assessment of the environmental effects of solid rocket effluents. The dispersive description accorded by the Multilayer Diffusion Model is initiated at the point where the ground cloud of exhaust effluents reaches thermodynamic equilibrium with the environment; and, therefore, this description depends strongly on the kinematic and thermodynamic profiles of the atmospheric conditions along with a knowledge of the chemistry and thermodynamics of the exhaust effluents present in this cloud.

The initial considerations in this section are given to the review of the techniques for establishing the spatial location of the ground cloud equilibrium (see Symbols and Definitions). Secondly, a general summary of the Lagrangian dispersion of a volume source is given as an introduction to the relevant diffusion descriptions for the Titan effluents accorded by the NASA/MSFC Multilayer Diffusion Model. (A general description of this NASA model is given in Appendix B.) Then the assumptions that are utilized in the NASA/MSFC Surface-Layer Diffusion Model for real-time predictions are given. The significant mathematical expressions supporting these discussions have been included in Appendices A, B, and C. Appendix D gives the toxicity standards for the effluents from the Titan III.

A. Altitude of Cloud Equilibrium

The effluent cloud rise relations are employed to determine at what altitude the ground cloud reaches thermodynamic equilibrium (cloud stabilization) with the environment. The location of this altitude is significant since this point serves as the origin of the dispersive description. This equilibrium point is chosen as the origin in order to eliminate complex thermodynamic considerations — thus, limiting the diffusion problem to solely kinematics [3].

The burning of rocket solid motors results in the formation of a cloud of hot exhaust products which subsequently rises and entrains ambient air (99.9 percent air) until a thermodynamic equilibrium with ambient conditions is attained. For normal launches, this cloud is formed principally by the forced ascent of hot turbulent exhaust products that have been deflected laterally and vertically by the launch pad hardware and the ground surface. The height at which this ground cloud stabilizes is determined by the vehicle type — in this case the Titan IIIC — and atmospheric stability. The vehicle type determines whether a continuous or instantaneous source model is required. In the <u>instantaneous source model</u>, spherical entrainment is assumed; that is, the entrained ambient air enters the exhaust cloud uniformly from all directions. In the <u>continuous source model</u>, cylindrical entrainment is assumed; that is, the entrained ambient air enters the cloud uniformly only on the sides of the cylinder and not the ends. Thus, this terminology — continuous or instantaneous source — in reference to the cloud rise model does not directly imply the duration of the exhaust cloud, as it does in the diffusion model, but only implies the form of the entrainment process. The entrainment process is a function of the residence time of the vehicle on the pad. Experience to date indicates that the buoyant rise of exhaust clouds from normal launches of <u>solid-fueled vehicles</u> such as the Titan III is best predicted by using a cloud rise model for instantaneous sources [4]; the cloud rise for <u>large liquid-fueled</u> vehicles is best predicted by the use of a cloud rise model for <u>continuous sources</u> [5, 6, 7]. While no cloud rise data are available for on-pad aborts, cloud rise data from static tests of liquid-fueled rockets indicate that the use of a cloud rise model for continuous sources is appropriate for a slow conflagration of the vehicle. Because the scope of this discussion is restricted to the normal launch of a Titan IIIC, detailed considerations of the exhaust cloud rise relations in Appendix A are restricted to the instantaneous source.

The exhaust cloud rise model for an instantaneous source has two formulations in accord with the atmospheric temperature lapse rate. This model assumes that the atmosphere is either quasi-adiabatic or stable. Here the quasi-adiabatic is where the adiabatic atmosphere is the limit, which means that the potential temperature difference ($\Delta\Phi$) — which is a measure of the entropy change in the atmosphere — is zero or less, where the potential temperature difference is given by

$$\Delta\Phi = \Phi_z - \Phi_R \quad , \tag{1}$$

where Φ_z and Φ_R are the potential temperatures at some height z and at the surface reference. The potential temperature (Φ) is defined as

$$\Phi = T\left(\frac{1000}{p}\right)^{0.288} \tag{2}$$

where T is the temperature at an altitude whose corresponding pressure is p, Φ is the temperature that a volume of air would have if it were adiabatically (no heat transfer) compressed (or expanded) from p to 1000 millibars. If this potential temperature difference is positive, then the atmosphere is treated as stable because there is an entropy increase with altitude. Since in most cases of interest there will be an inversion layer present, the stable cloud rise formula is the relation normally utilized to determine the equilibrium height of the exhaust cloud. Here a balance between the exhaust cloud entropy and the atmospheric entropy is achieved.

B. Generalized Diffusion Model

The generalized diffusion model describes the kinematic transport — in terms of the temporal and spatial levels of concentration and dosage — of the exhaust constituents assuming the effluents in the cloud are in thermodynamic equilibrium with the environment. A Lagrangian model is assumed, where volumetric cloud expansion is about a reference point moving at the average velocity of the homogeneous fluid. For diagnostic and interpretative flexibility in this discussion, this model will be formatted in a modular form for both concentration and dosage; and since the diffusion algorithms for the spatial concentration are an extension of the dosage algorithm (Appendix B), the modular form of the dosage is considered first.

The generalized dosage model for a nearly instantaneous source is defined by the product of four modular terms:

$$\text{Dosage} = (\text{Peak Dosage Terms}) \times (\text{Lateral Term}) \times (\text{Vertical Term}) \times (\text{Depletion Term});$$

whereas, the generalized concentration model for a nearly instantaneous source is expressed as the product of five modular terms:

$$\text{Concentration} = (\text{Peak Concentration Term}) \times (\text{Along-Wind Term}) \times (\text{Lateral Term}) \times (\text{Vertical Term}) \times (\text{Depletion Term}) \quad .$$

These mathematical descriptions for the dosage and concentration models permit flexibility in application to various sources and for changing atmospheric parameters by maintaining a rigorous mass balance.

Two obvious differences exist between the dosage and concentration models. First, the peak concentration term refers to the concentration at the point x, y = 0, z = H (where x is along the wind direction and H is any height) and is defined by the expression

$$\text{Peak Concentration} = \frac{Q}{(2\pi)^{3/2}\sigma_x\sigma_y\sigma_z} , \tag{3}$$

where Q is the source strength and σ_i is the standard deviation of the concentration distribution in the ith direction; whereas, the peak dosage term is given by

$$\text{Peak Dosage} = \frac{Q}{2\pi\,\bar{u}\,\sigma_y\sigma_z} , \tag{4}$$

where $\bar{u}$ is the mean wind speed over time and space. The second difference between these models is that the concentration contains a modular along-wind term to account for downstream temporal effects not considered in the dosage model. The along-wind term affords a Gaussian decay in the concentration as a function of cloud transit time and the mean wind speed for the concentration distribution.

The lateral term, common to both models, is another Gaussian term which is a measure of the number of lateral standard deviations away from the centerline of the calculation. The lateral standard deviation is a function of the lateral diffusion coefficient and the variance in the horizontal wind azimuth. The vertical term, common to both models, is similar to the lateral term except that the vertical components are utilized and reflection is accounted for at the top and bottom of the layer.

The last modular in both models is the depletion term. This term accounts for the loss of material by simple decay processes, precipitation scavenging, or gravitational settling. While this option exists in the NASA/MSFC Multilayer Diffusion Model, the depletion function will not be utilized for the Titan III exhaust modeling of this launch. Since each of the modular terms in these general relations is dependent upon empirical parameters that can only be determined from actual solid rocket launches, it is incumbent to perform reliable measurements of the dispersive transport from the effluent for as many solid rocket launches, such as the Titan III, as possible to insure maximum reliability in these empirical diffusion parameters. This will in turn afford a more accurate diffusion description from the model for Shuttle launches.

C. Real-Time Diffusion Prediction

A spatial description of the concentration and dosage fields resulting from the launch of a Titan III vehicle has been developed which affords real-time diffusion predictions by specialization of Model 3 in the NASA/MSFC Multilayer Diffusion Model (Appendix B) [1]. The primary function of these real-time diffusion predictions is to estimate the HCl concentration fields prior to launch, from a meteorological forecast, for the deployment of instrumentation to monitor the transport of the exhaust effluents from the solid rocket motors which are released during the launch of a Titan III. These predictions are made on a portable programmable desk calculator (HP 9820) at Cape Canaveral.

These diffusion predictions include graphical descriptions for: (1) the forecasted atmospheric profile at launch time, (2) the temporal exhaust cloud rise history, (3) the centerline concentrations and dosage profile for HCl along the cloud's transit path, and (4) the HCl concentration isopleths. The meteorological profile gives the delineations for the kinematics and thermodynamics of the first 2 km of the atmosphere along with the values for the surface density, pressure, and temperature. Both the dry bulb temperature and the potential temperature profiles are given. The dry bulb temperature profile is given as a guide to layering, since it clearly shows inversions and isothermal layers. The potential temperature, which is the pressure-normalized dry bulb temperature [equation (2)], gives a relative measure of the atmospheric entropy and is the fundamental parameter in determining the height of the cloud stabilization where the exhaust cloud is in equilibrium with the atmosphere. Since the type of atmosphere — adiabatic or stable — determines the cloud rise relation that is employed, the potential temperature profile affords a quick-look procedure for this thermodynamic classification of the atmosphere as a function of altitude. (Potential temperatures that fall to the left of the vertical line through the surface potential temperature are in the superadiabatic regime, while those to the right are in the stable regime.) The temporal history of the ascent of the exhaust cloud gives the time and height of cloud stabilization. This graph also shows the atmosphere regimes which were adiabatic and stable.

The remaining two graphical descriptions utilized the specialized version of the NASA/MSFC Multilayer Diffusion Model which we will refer to as the NASA/MSFC Surface-Layer Diffusion Model (mathematical considerations are given in Appendix B) since it considers only the kinematic effects in the surface mixing layer. The Surface-Layer Diffusion Model is designed to give the predicted concentrations and dosages at the surface. This model assumes that the standard deviations in the temporal fluctuations of the wind direction in elevation and azimuth are the same and that the diffusion coefficients are one — otherwise, this model is the same as Model 3 in the Multilayer Diffusion Model. This specialized diffusion model is employed in determining the centerline concentrations and dosages of HCl for the first 20 km after cloud stabilization. (Note: All distances on this figure are measured from the point of cloud stabilization and not from the launch site.) This graph also gives the values for the maximum concentration and the height of the surface mixing layer. The option exists to retrieve the surface cloud size and passage times along this cloud path.

The final graphical description is normally superimposed on a map of the Cape Canaveral area and shows the HCl concentration isopleths along with the exhaust cloud path. The points at which cloud stabilization and the maximum concentrations occurred are shown along with their corresponding cloud passage times after launch. An additional time mark is given so that the cloud passage time can be determined for any point after cloud stabilization values for the location relative to the launch sites of the point of maximum concentration along the time of occurrence are printed out.

It should be emphasized that the accuracy of the real-time diffusion predictions depends very strongly on the meteorological forecast used. The most critical parameter in this forecast relative to the deployment of a monitoring matrix is the wind direction. Results of these predictions are considered in the next section.

SECTION III. DIFFUSION PREDICTIONS FOR THE TRANSPORT OF THE SOLID ROCKET MOTOR EXHAUST EFFLUENTS FROM THE LAUNCH OF A TITAN IIIC VEHICLE

J. Briscoe Stephens, Leonard L. DeVries,
C. Kelly Hill, and Michael Susko

Predictions of the surface concentration and dosage fields of the potentially toxic constituents in the exhaust effluents of the Titan IIIC vehicle, which was launched from the Eastern Test Range at Cape Canaveral Air Force Station at 1857 EST on December 13, 1973, are discussed here. These predictions include both the forecasted diffusion predictions and the launch diffusion prediction obtained with the NASA/MSFC Surface-Layer Diffusion Model [1] along with the launch predictions obtained with the NASA/MSFC Multilayer Diffusion Model [2]. Because these predictions were in support of a ground measurements program, the primary emphasis in these predictions was directed toward surface effects.

The two basic kinds of input parameters required for diffusion predictions are (1) the chemical and thermodynamic characteristics associated with the vehicle exhaust products and (2) the atmospheric conditions into which these exhaust products are being released. Therefore, the characteristics of the Titan III exhaust effluents will be initially considered followed by the meteorological conditions as an introduction to the launch diffusion predictions. These launch predictions will be utilized as baseline in the discussion of the forecasted diffusion predictions.

A. Chemical and Thermodynamic Characteristics of the Titan III Exhaust Effluents

To ascertain the height and composition of the stabilized exhaust cloud from the Titan III, an inventory of the chemical and thermodynamic properties of the Titan III exhaust effluents is necessary since they constitute or dictate the source input parameters to the NASA/MSFC Multilayer Diffusion Model.

The existence of a low altitude exhaust cloud, resulting from the launch of a Titan rocket, has been observed and is theoretically predicted. This exhaust cloud is comprised of less than 1 percent rocket exhaust effluents and more than 99 percent entrained air and will normally stabilize at an altitude somewhere between 500 m and 1500 m. The solid rocket motor effluents (Table 1) include hydrogen chloride, carbon monoxide, alundum, nitrogen, water vapor, carbon dioxide, hydrogen, and nitrogen monoxide. Our interest here is directed toward hydrogen chloride, carbon monoxide, alundum, and

TABLE 1. FUEL PROPERTIES OF THE TITAN IIIC ZERO-STAGE ENGINES[a]

Fuel Emission Factors (Fraction by Weight)		
Hydrogen Chloride	HCl	0.210
Carbon Monoxide	CO	0.279[b]
Alundum	Al_2O_3	0.304
Nitrogen	N_2	0.084
Water Vapor	H_2O	0.067
Carbon Dioxide	CO_2	0.029
Hydrogen	H_2	0.025
Nitrogen	NO	0.0002
Fuel Expenditure Rate		
$\dot{W} = 4.174 \times 10^6$ g/sec		
Fuel Heat Content		
q (dry) = 691 cal/g		
q (water) = 608 cal/g		

a. Information supplied by A. E. Weller of Battelle Columbia Laboratories.
b. May be converted to CO_2.

carbon dioxide, since these are the potentially toxic constituents (Appendix D) which could result in adverse impacts if exposures to high concentrations of these effluents occurred.

A logarithmic least-squares regression analysis of the Titan III fuel expenditure data was utilized to determine the relationship between the vehicle ascent time (t_R: sec) and the vehicle altitude (z_R: m) [4], which is

$$t_R = 0.63463\, z_R^{0.4837} \quad .$$

Based on the Titan fuel expenditure rate ($\dot{W} = 4.174 \times 10^6$ g/sec), the fuel expenditure (W: g) as a function of altitude is

$$W = 2.648946 \times 10^6 \ H^{0.4837} \quad ,$$

where H is the height of cloud stabilization. To obtain the amount of a constituent in this source, the fractional percent by weight associated with the constituent, which is given in Table 1, is mulitplied by the total fuel expenditure (W) for the surface mixing layer.

To obtain the amount of heat present in the rocket exhaust, which determines the exhaust cloud stabilization height, a fuel heat constant (q: cal/g) must be determined. The normal fuel heat constant associated with the Titan IIIC rocket fuel is 960 cal/g of fuel expended. This heat constant assumes a release of exhaust effluents into dry air. When Titans are launched from the Eastern Test Range, water is sprayed on the launch pad. According to H. E. Eley, Aerospace Corporation, a total of 209 000 gal of water was released on the pad and all but 27 600 gal could be accounted for after the launch of the Titan IIIC on December 13, 1973 (Table 1). Thus we assumed that most of this 27 600 gal of water was vaporized by the heat of the rocket exhaust; therefore, this heat loss is reflected in the value of the fuel heat content we use. This corrected fuel heat content is 607.754 cal/g of fuel for this launch. Then, the Titan heat released (Q: cal) is

$$Q = 1.609907 \times 10^9 \ H^{0.4837}$$

for a cloud stabilization height of H. This value was employed in our cloud rise calculation (Appendix A).

This Titan exhaust was not photographed because the launch was at night; therefore, a direct comparison of our results for cloud growth as a function of cloud rise cannot be made. However, these relations have been tested during other launches.

B. Meteorological Conditions

Meteorological forecasts for the atmospheric conditions at launch time (1857 EST, December 13, 1973) were made every few hours during the day preceding the launch. These forecasts of the wind kinematics and the atmospheric thermodynamics were utilized to make predictions of the dispersive transport of the exhaust effluents for the deployment of the monitoring network. The parametric data used in these forecasts were obtained from rawinsonde soundings and meteorological towers located around the launch site. These data were employed in conjunction with routine regional and national synoptic weather charts to provide the forecast of the necessary atmospheric parameters for the NASA/MSFC Multilayer Diffusion Model. Preliminary forecasts for the diffusion predictions were made as early as 1 week prior to the launch. During the last 8 hours prior to launch, the diffusion predictions were made approximately every 2 hours. The diffusion prediction made 6 hours prior to the launch was critical for the deployment of the monitoring network, and the diffusion prediction made 1 hour prior to the launch was critical for determining the period of operation for the monitoring instrumentation.

The atmospheric profiles for the wind velocity, dry bulb temperature, and potential temperature at approximately launch time obtained from a rawinsonde sounding released from the Cape Canaveral Weather Station at 1901 EST is shown in Figure 1. Since the rawinsonde is released at a site about 10 km from Complex 40 where the Titan was launched, the surface conditions utilized are taken from the meteorological tower (110) located between the two Titan launch complexes (Complexes 40 and 41). The continuous monitoring

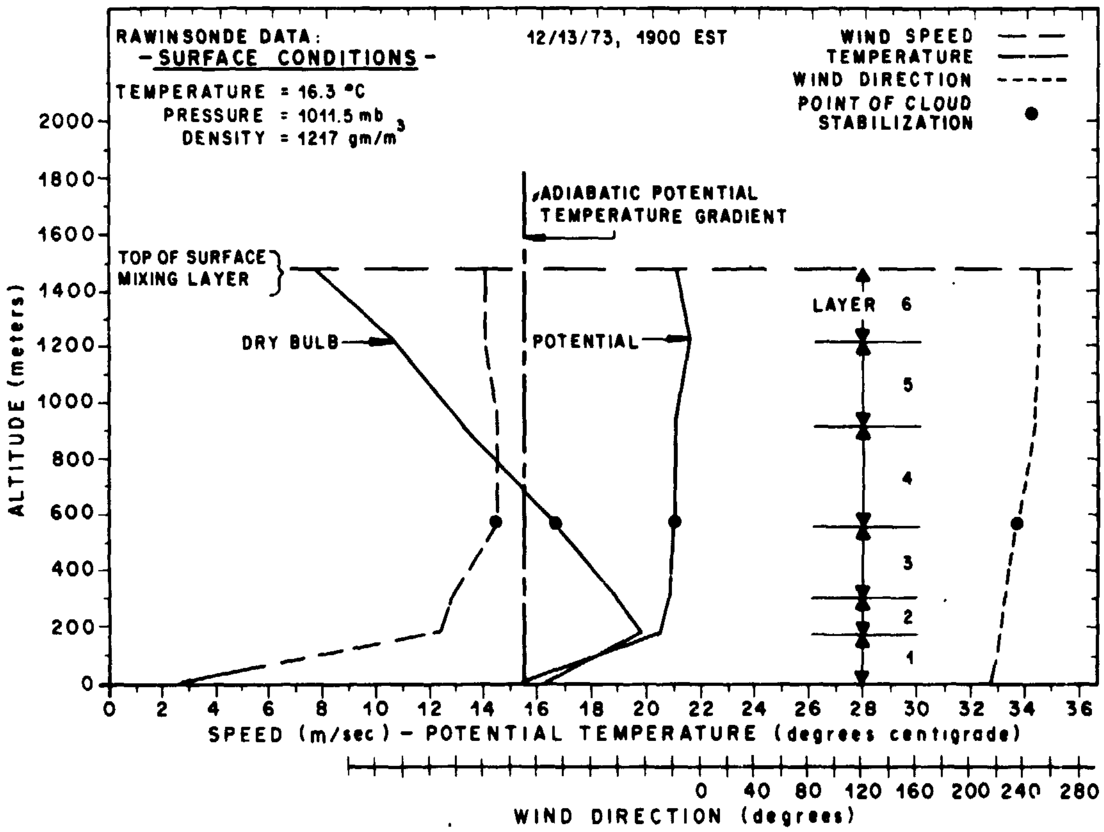

Figure 1. Atmospheric conditions at launch time (T-0).

of the meteorological conditions at NASA's 150-m Ground Wind Tower on Merritt Island provided information that was helpful in noting critical trends in the lowest layers of the atmosphere during the periods between rawinsonde soundings. Fair weather persisted over the region at launch time. A surface high pressure system developed over Texas several days earlier and moved slowly along the Gulf States to be centered over Florida at 0700 EST (1200Z), December 13, 1973, as shown in the synoptic weather chart (Fig. 2). This surface synoptic weather chart, although prepared 14 hours prior to launch time is representative and did not change radically through the time of launch. Surface pressure values within this high pressure weakened ste 'ily, and by launch time the system had moved eastward away from Florida and lost identity. The weather pattern over Florida was being replaced at launch time by southwesterly flow associated with the approaching cold front that had moved into extreme northern Florida by launch time.

The T-6 forecast (Fig. 3), which was made 7 hours preceding the launch, agreed overall rather well with the rawinsonde sounding at launch. The wind direction prediction varied approximately linearly with altitude from 220 deg at the surface to 252 deg at an altitude of 1500 m compared with the actual wind direction at launch of 210 deg at the surface to 243 deg at an altitude of 1450 m – that is about a 10-deg difference between the two wind direction profiles. The forecasted temperature profile did not reflect the radiation inversion over the first 160 m that occurred at launch, which means that the predicted cloud stabilization height for the forecast will be higher than the actual height. There is about a 3 m/sec difference in wind speed which will affect the range out to the point of maximum concentration.

C. Input Parameters for the Diffusion Model

Based on the characteristics of the vehicle being launched – in this case the Titan IIIC – and the atmospheric conditions at the time of launch, a set of input parameters for the MSFC/NASA Multilayer Diffusion Model is defined. The atmospheric thermodynamics and kinematics are the primary variables in defining the spatial and temporal location of the exhaust cloud stabilization. Vehicle characteristics define the amount of entropy in the cloud and the size of the cloud.

The input parameters, except for the potential temperature gradient used to obtain the temporal history of the ascent of the Titan III exhaust cloud are given in Table 2. Since the potential temperature gradient ($\partial \Phi / \partial z = \nabla_z \Phi$) is a function of altitude, this must be obtained directly from the potential temperature profiles which are given in Figures 1 and 3. Because the residence time on the pad of the Titan is short, the instantaneous form of the cloud rise

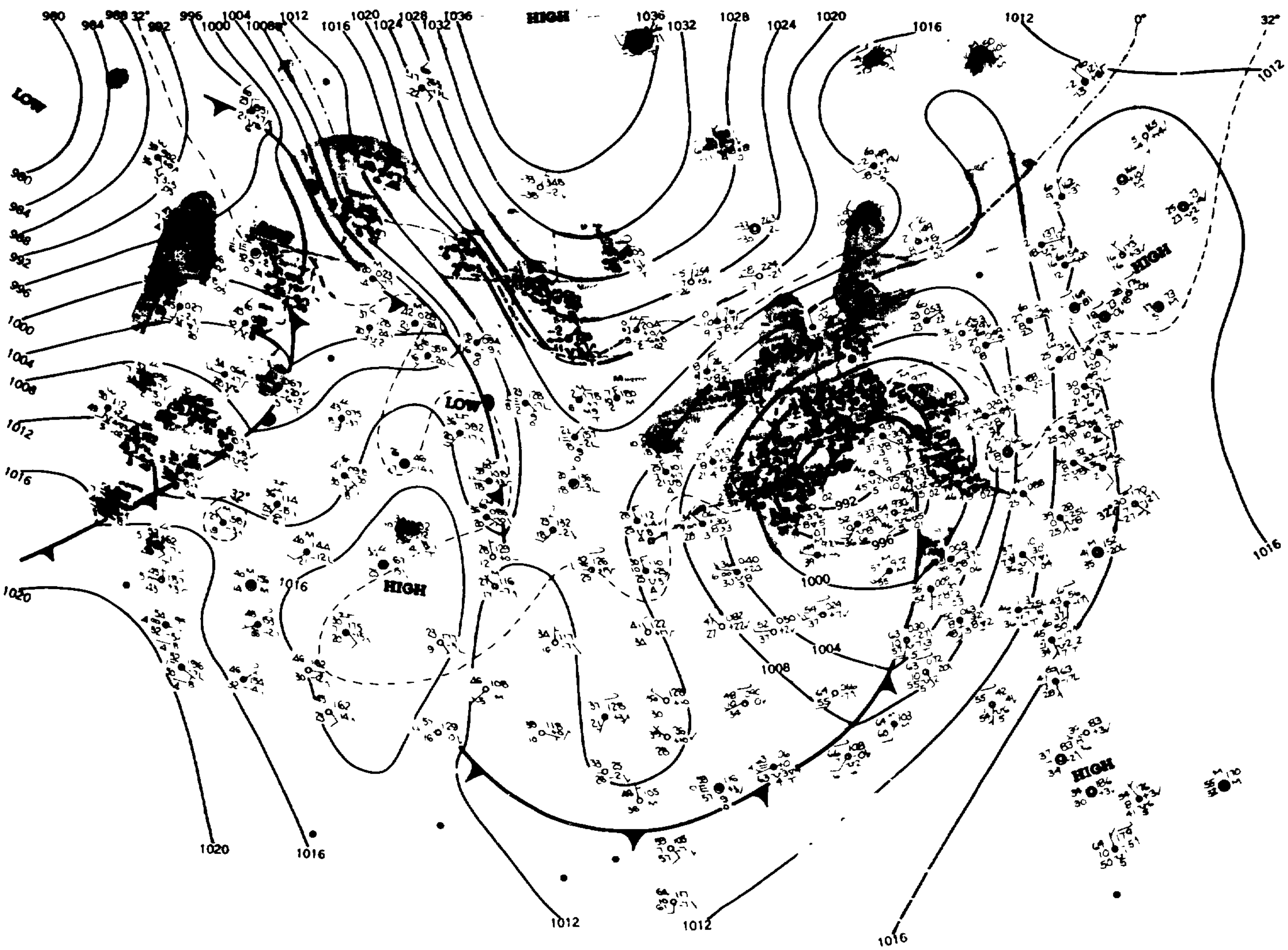

Figure 2. Surface synoptic weather map for launch day [0700 EST (1200Z), December 13, 1973].

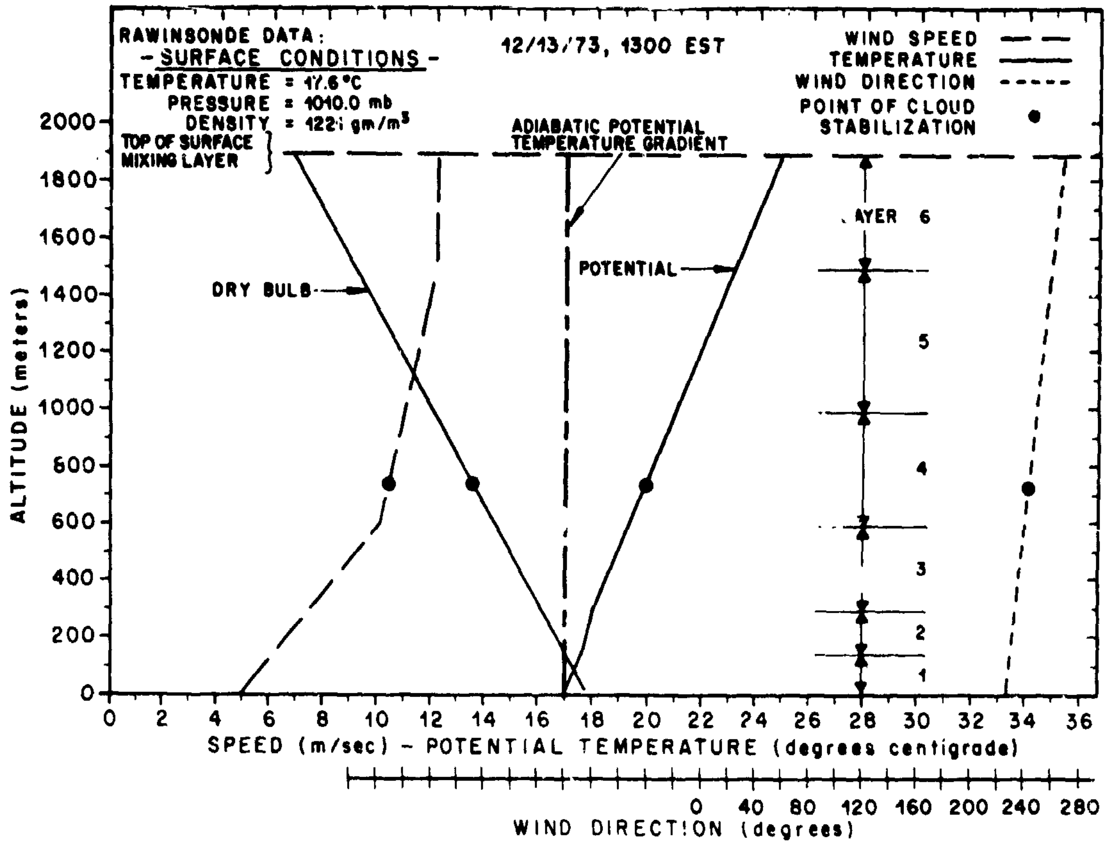

Figure 3. Forecast of atmospheric conditions for launch time made 6 hours prior to launch (T-6 hours).

formula [8] (spherical entrainment) given in Appendix A is used. Since the potential temperature gradient is positive in both the forecasted and launch profiles at all altitudes of interest, the stable cloud rise formula for an instantaneous source is used for this case. Using the values given in Table 2, the temporal form for the stable instantaneous cloud rise formula [equation (A-4)] can be expressed for the Titan IIIC as

$$t = \frac{\arccos\left[1 - \dfrac{4.846391298\,\nabla_z \Phi\, z^{3.5163}}{T_s^{\,2} \rho_s}\right]}{\dfrac{9.8\,\nabla_z \Phi}{T_s}}, \qquad (5)$$

TABLE 2. INPUT PARAMETERS FOR CLOUD RISE FORMULA

A. Titan IIIC Characteristics			
1. Heat released: $Q = 1.609907 \times 10^{9} H^{0.4837}$ cal			
2. Initial cloud radius: $r_R = 0$			
3. Entrainment constant [9]: $\gamma = 0.64$			
4. Specific heat of air: $c_p = 0.24$ cal/g °K			
5. Initial vertical velocity: $W_o = 0$			
B. Meteorological Elements			
		Forecasted (1300 EST)	Measured (1900 EST)
1. Air density	ρ	1221 g/m³	1217 g/m³
2. Ambient temperature	T	290.75°K	289.45°K

where t(sec) is the time for the exhaust cloud to rise to an altitude z(m). T_s and ρ_s are the surface temperature and density. The potential temperature gradient $(\nabla_z \Phi)$ is the difference between the potential temperature at an altitude z and the surface. The altitude for cloud stabilization (H) is the value of z that results in the argument of the arc cosine equaling a minus one.

The temporal history of the ascent of the Titan IIIC exhaust cloud for the atmospheric condition at launch time is shown in Figure 4, and the temporal history for the T-6 forecasted atmospheric conditions at launch time is shown in Figure 5. These results suggest that the exhaust cloud would have reached thermodynamic equilibrium with the atmosphere 149 sec after launch, with the center of mass of the exhaust cloud located at a stabilization height of 560 m. The relationship between this cloud height (H) and the exhaust cloud radius (r) is

$$r = \gamma H \quad , \tag{6}$$

where γ is the entrainment coefficient. This means that the cloud radius was 358 m at cloud stabilization. The predicted values based on the T-6 forecast were a rise time of 248 : at a stabilization height of 730 m. The difference

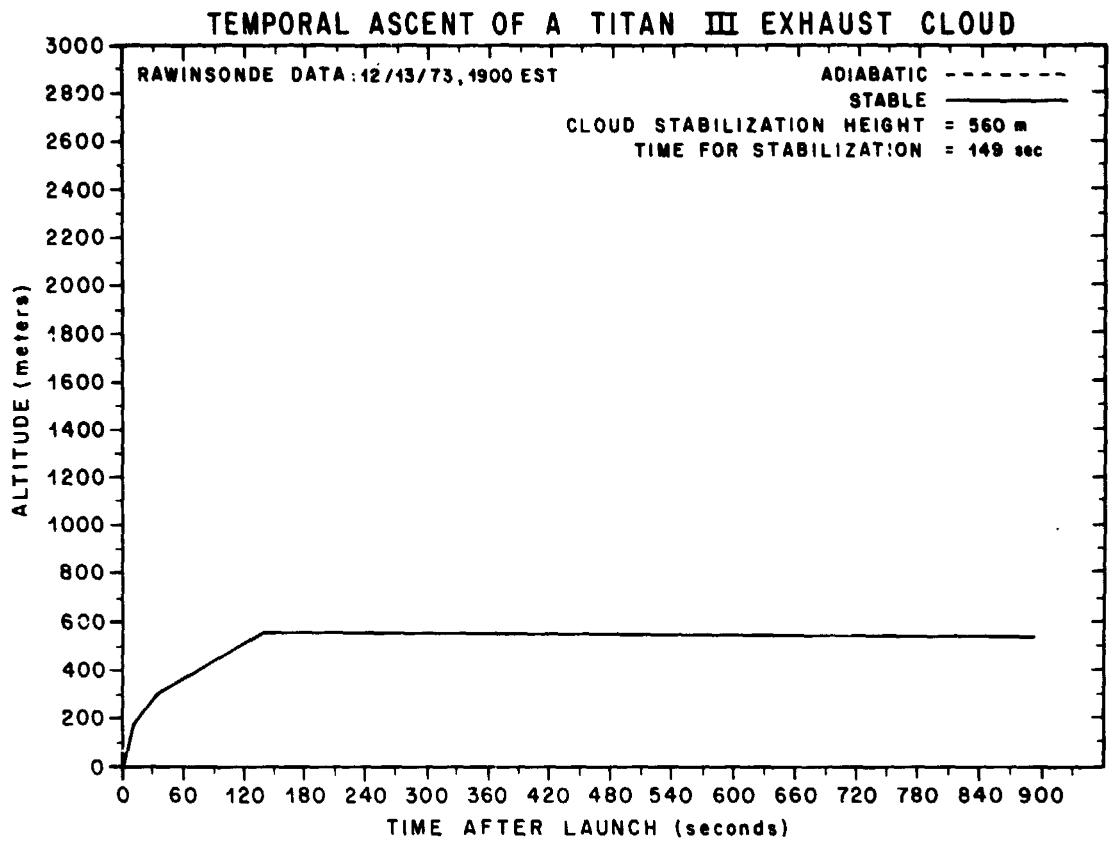

Figure 4. Predicted exhaust effluent cloud rise history for launch atmosphere (T-0).

between the launch and the forecasted predictions for the cloud stabilization parameters is due largely to the fact that the radiation inversion was not forecasted. This might have been avoided by a T-24 hour rawinsonde sounding. It should be noted, however, that in spite of the 30-percent difference in stabilization height, in this case the concentration fields, as will be seen in the next part, were not significantly different between the forecast and launch predictions.

The top of the surface mixing layer at launch time was about 1450 m, whereas we had used 1900 m in our T-6 hours forecast. This difference had very little effect on the diffusion predictions. In both cases we did use the same value of 7 for the standard deviation in the mean wind azimuth at the surface (σ_{AR}).

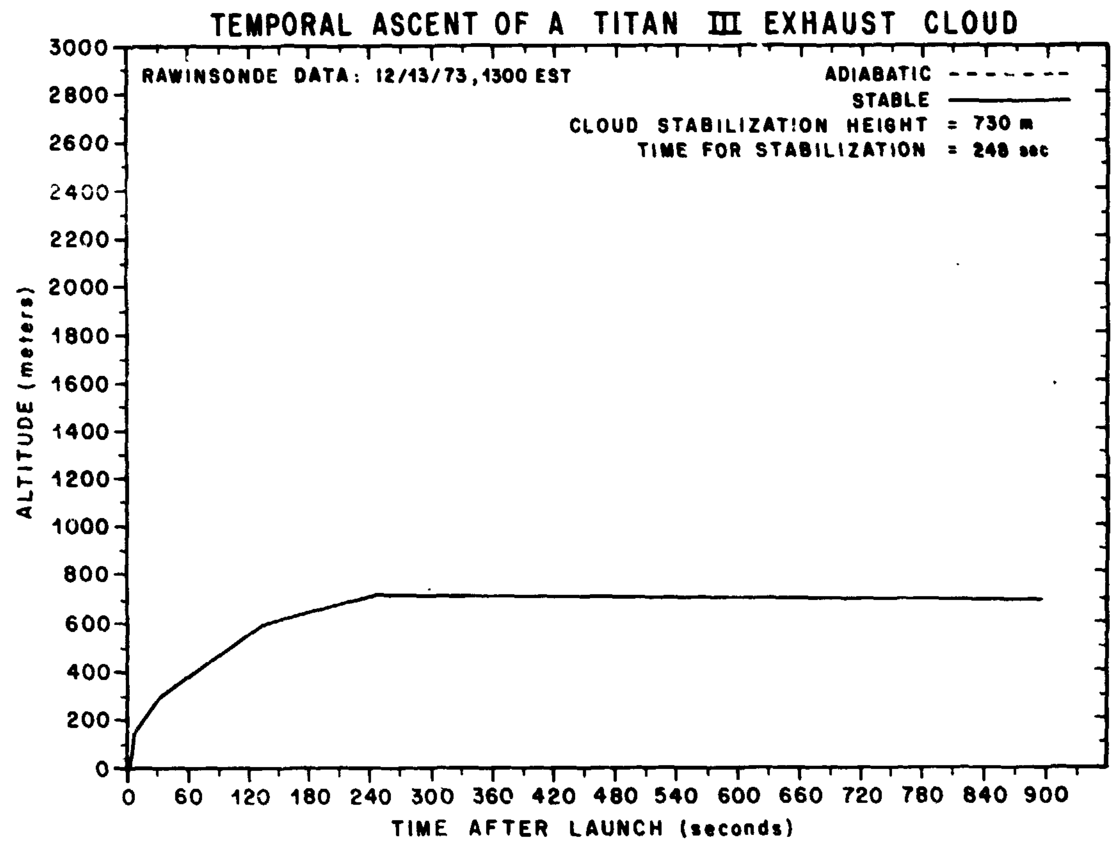

Figure 5. Predicted exhaust effluent cloud rise history forecasted 6 hours prior to launch (T-6 hours).

Since there was a requirement for the definition of the near field concentrations of HCl, Model 4 was used. This required the layering of the surface mixing layer. The layering is shown on the respective atmospheric profile in Figures 1 and 3. This layering was selected both to reflect the changes in atmospheric gradients and to ensure a reasonable distribution of the source material in Model 4.

D. Predictions for the Concentrations of Exhaust Effluents from the Launch of the Titan IIIC

The predictions for the dispersion of the exhaust effluents from the launch of the Titan IIIC on December 13, 1973, at 1857 EST from the Eastern Test Range at Cape Canaveral Air Force Station will be considered. While results for all the potentially toxic rocket exhaust constituents — hydrogen chloride (HCl), carbon monoxide (CO), carbon dioxide (CO_2), and alumina (Al_2O_3) — will be summarized based on the atmospheric condition at launch time, only the results for hydrogen chloride will be given (leaving the other constituents for the reader to extrapolate if needed) for the T-6 hours forecast for the atmospheric conditions at launch time.

The diffusion predictions for this launch were made in real time on-line at the Range Control Center for the Eastern Test Range on a programmable desk calculator by Marshall Space Flight Center and H. E. Cramer Company personnel using the NASA/MSFC Surface-Layer Diffusion Model. Simultaneously, at Marshall Space Flight Center, the same diffusion predictions were being run on the computers with the NASA/MSFC Multilayer Diffusion Model for use as backup information and to provide a more detailed analysis. The online calculator results were designed to afford Langley Research Center real-time graphical results which they could use to define their exhaust monitoring grid. The computer results obtained at Marshall Space Flight Center were utilized as a check on the online results and are valuable in the postlaunch analysis. The online results employed primarily Model 3 of the NASA/MSFC Multilayer Diffusion Model; however, the computer results are for both Model 3 and 4. Model 3 is probably the best model to use with a forecasted atmospheric profile since this model treats the surface mixing layer in terms of the average kinematics. The primary disadvantage of this model is that it does not provide a description of the effluent transport prior to cloud stabilization. Model 4, on the other hand, can be used to obtain a description which accounts for the small tail of the exhaust cloud that tends to initially remain on the surface. This model allows the scientist more freedom to model the detailed atmospheric conditions that are reflected in a rawinsonde sounding. Unfortunately, the storage requirements for plotting the isopleths using Model 4 are so great that these calculations must be done on a computer. Since the results from Model 3 and Model 4 are about the same after the peak concentration in Model 3, we feel that Model 3 is more than adequate for online calculations; however, more comparison with empirical results is required to justify this conclusion.

The launch diffusion predictions for Model 3 are based on the atmospheric profile shown in Figure 1 and the cloud ascent history shown in Figure 3. The layering parameters used for the launch diffusion predictions in Model 4 are given in Tables 3 and 4. The predictions for the centerline concentration and dosage of hydrogen chloride (HCl) using Model 3 are presented in Figure 6, and those using Model 4 are presented in Figure 7. The distances for the Model 3 calculations are measured from the point of the exhaust cloud stabilization, which was 1792.6 m from the launch complex (Complex 40) at a direction of 49.06 deg. The Model 4 distances are measured — as will be explained — from the launch complex. The maximum concentration of HCl for Model 3

TABLE 3. METEOROLOGICAL MODEL INPUTS FOR THE SIX LAYERS

Parameter	Units	Layer 1	2	3	4	5	6
$\bar{u}_R$	m sec^{-1}	3.6					
$\bar{u}_{BK}$	m sec^{-1}	5.0	12.3	12.8	14.4	14.4	1[illegible].9
$\bar{u}_{TK}$	m sec^{-1}	12.3	12.8	14.4	14.4	13.9	13.9
θ_{BK}	°K	210.0	217.0	220.0	229.0	240.0	244.0
θ_{TK}	°K	217.0	220.0	22[illegible].0	240.0	244.0	243.0
$\sigma_{AR}\{\tau_{oK}\}$	deg	7.00					
$\sigma_{ABK}\{\tau_{oK}\}$	deg	7.00	3.02	2.64	2.28	2.03	1.90
$\sigma_{ATK}\{\tau_{oK}\}$	deg	3.02	2.64	2.28	2.03	1.90	1.81
τ_{oK}	sec	600	600	600	600	600	600
α_K		1.0	1.0	1.0	1.0	1.0	1.0

TABLE 4. SOURCE INPUTS FOR STABILIZED CLOUD

Parameter	Units	Layer 1	2	3	4	5	6
z_R	m	2					
z_{BK}	m	5	170	300	550	900	1200
z_{TK}	m	170	300	550	900	1200	1450
τ_K	sec	168	168	168	168	168	168
$\sigma_{yo}\{K\}$	m	25.3	69.9	126.5	101.9	93.0	93.0
$\sigma_{xo}\{K\}$	m	25.3	69.9	126.5	101.9	93.0	93.0
Q_K	ppm m^{-1}	5.056×10^5	3.467×10^6	1.467×10^7	1.560×10^7	5.115×10^6	4.293×10^6

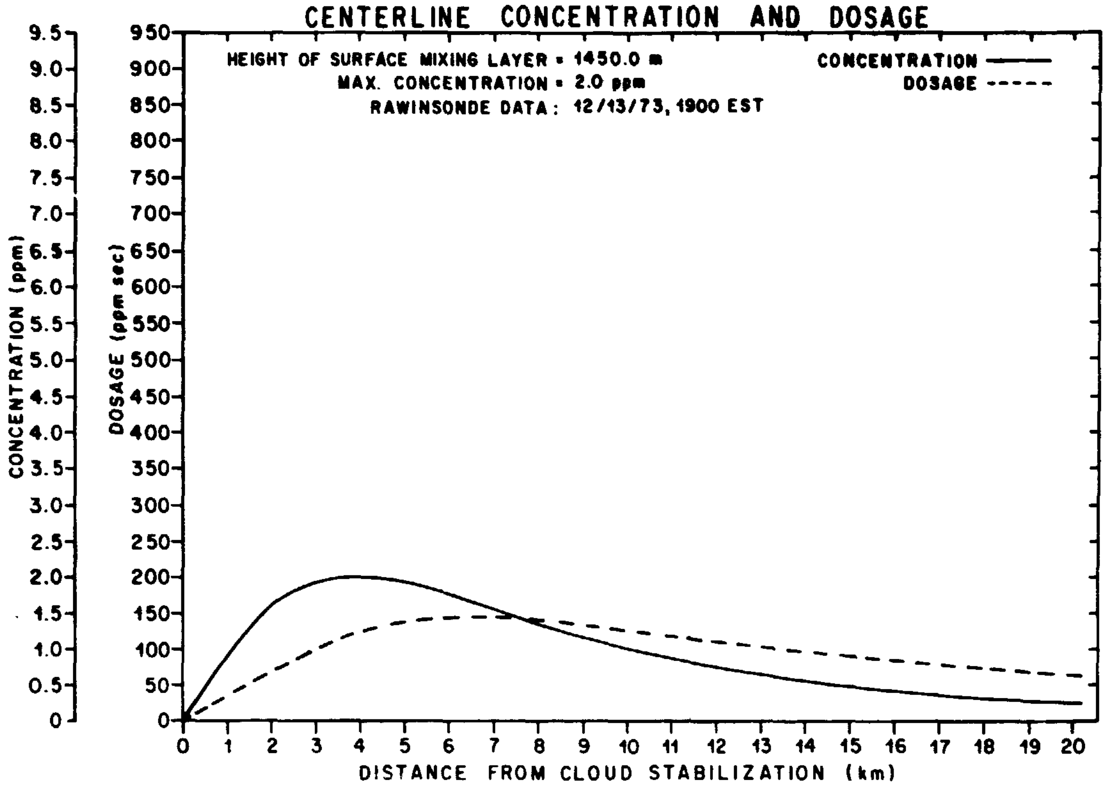

Figure 6. Model 3 launch prediction for the centerline concentrations and dosages (T-0).

occurs at approximately the same range as the relative maximum concentration (the first derivative is zero and the second derivative is negative) for Model 4 in accordance with the above definitions for the model origins. The relative maximum concentration (Model 4) is 30 percent less than the maximum concentration (Model 3) which is reasonable since the diffusion in Model 4 is initiated at the launch complex rather than at cloud stabilization as is done in Model 3. Before addressing the near field differences between these models, the isopleths (contours of constant concentration) for HCl must be examined.

The HCl isopleths based on the atmospheric condition at launch time (1857 EST) are presented for Model 3 in Figure 8 and for Model 4 in Figure 9. (The 1-ppm HCl isopleth is selected because this is the detection threshold for HCl measurement instrumentation such as a bubbler.) To compare these mappings, we will define the near field as the region between the launch complex and the point of maximum concentration in Model 3. The region beyond this point will be referred to as the far field.

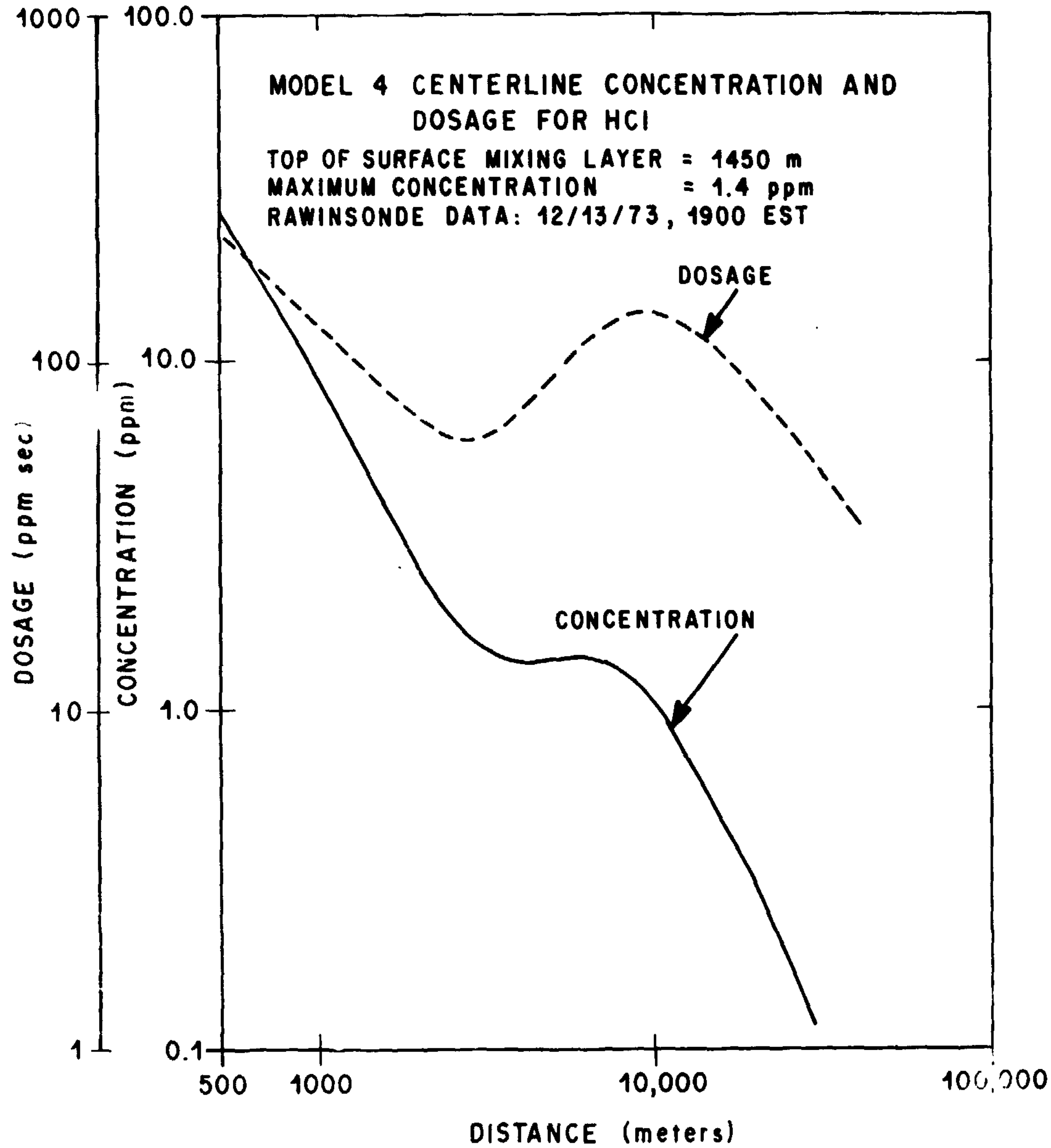

Figure 7. Model 4 launch predictions for the centerline concentrations and dosages (T-0).

In the far field the dimensions of the Model 3 and Model 4 1-ppm HCl isopleths are approximately the same. In the near field, there is considerable difference between the two models in accordance with the model definitions. Model 3 has assumed that all of the exhaust effluents rise to cloud stabilization. This assumption affords a very conservative estimate of the near field concentration levels from the exhaust effluents. Since observations of the Titan

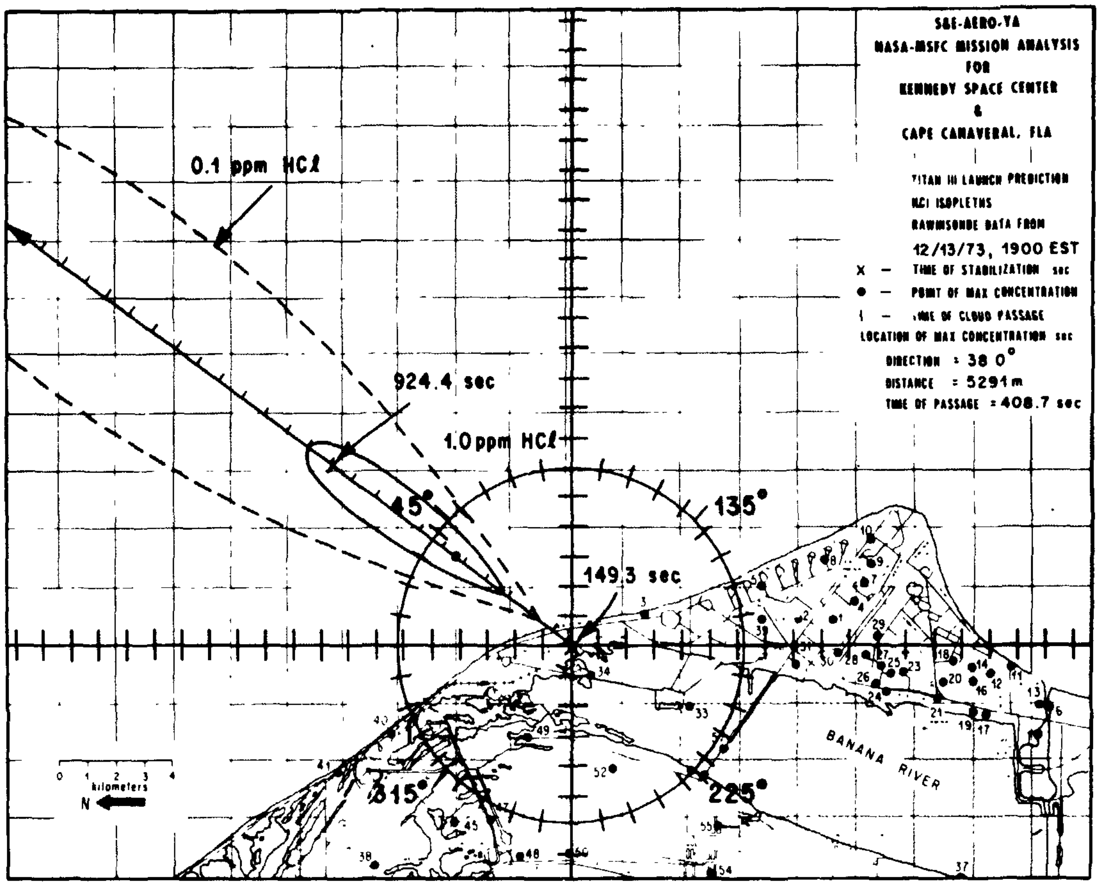

Figure 8. Model 3 launch prediction for the HCl isopleths (T-0).

launches suggest that some of the exhaust effluents are cooled by the water spray on the launch pad and do not join the main exhaust cloud, the layering concept in Model 4 is used to reflect this feature of the rocket exhaust diffusion process. This provides what we feel is only an estimate for the description of the diffusion process in the near field; however, there is a need for field measurements of these rocket effluents so that the modeling of the diffusion process can be optimized and confidence limits can be defined.

Other differences between the diffusion predictions afforded by Models 3 and 4 include the direction of cloud transport. Model 3 defines the transport direction in terms of the wind direction at the cloud centroid, which gives a transit direction of 38 deg in this case. Model 4, on the other hand, defines

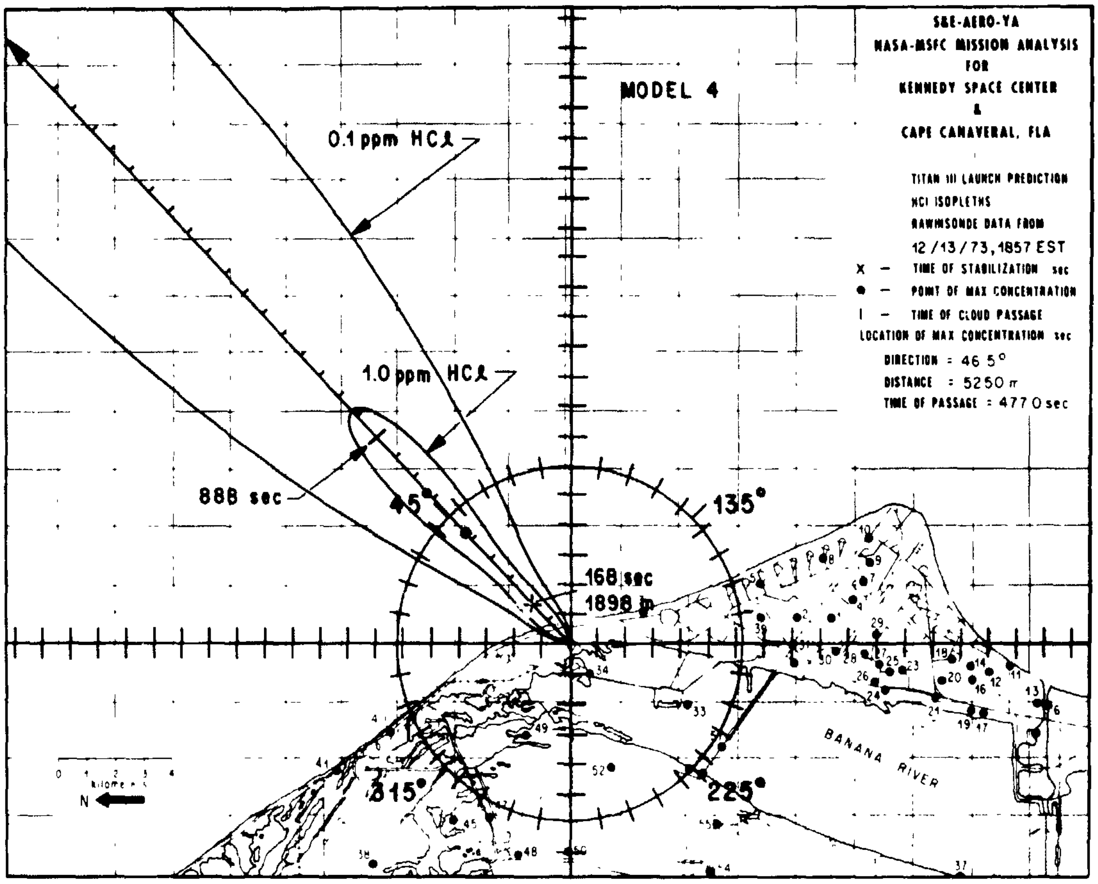

Figure 9. Model 4 launch predictions for the HCl isopleths (T-0).

the transport direction in terms of the mean wind direction in the surface mixing layer, which gives a transit direction of 46.5 deg in this case. This is 4.7 percent of the maximum difference (the maximum difference between two wind directions is 180 deg). Again, this is another example of where there is a need to develop a statistical inventory of field experience with rocket launches to resolve the optimum prediction techniques.

The concentration fields of the other Titan exhaust constituents, such as carbon monoxide (CO), carbon dioxide (CO_2), and alumina (Al_2O_3), are multiples of hydrogen chloride in these worst case calculations. These constants are:

Carbon monoxide: 1.73

Carbon dioxide: 0.11

Alumina: 2.22

This means that the 1-ppm HCl isopleth is also the 1.73-ppm CO isopleth, the 0.11-ppm CO_2 isopleth, and the 2.22-mg/m^3 Al_2O_3 isopleth. This also applies to dosages.

Langley Research Center had four instrumented sites approximately 1 km downstream of the launch complex. According to the Model 3 diffusion predictions, the amount of HCl should have been undetectable because these sites were before the exhaust cloud stabilization at 1.8 km (Table 5). (The basic assumption in this model is that the effects in this region are so small that they can be neglected.) The surface estimates for the exhaust cloud transit times and surface length are given in Table 5 based on the Model 3 predictions. An estimate for the description of the near field is probably afforded by Model 4 since the surface mixing layer was layered such that the first layer contained about 1.2 percent of the exhaust effluents contained in the surface mixing layer. About 97 percent of the effluents were assumed to be initially Gaussianly distributed on the surface in a circle with a diameter of 108.8 m. The results of the diffusion predictions for these parameters are given in Table 6.

The forecast of launch atmospheric conditions made 6 hours prior to launch (T-6 hours) given in Figure 3 afford Model 3 the centerline concentrations and dosages presented in Figure 10 and the HCl isopleths presented in Figure 11. These results compare well with the launch predictions. The predictions of the centerline concentrations and dosages are reasonably close. The maximum concentration in the forecast is 10 percent less than at launch. This may be a surprise in view of the differences in the cloud stabilization heights. The reason for this is that the depth of the surface mixing layer used for the forecast prediction (T-6 hours) was much greater than the depth used in the launch prediction (T-0) which results in less wind shear at launch time. This can be seen in the fatter isopleth in the forecasted prediction.

The range of the maximum concentration differed by 15 percent between the Model 3 forecast and the launch prediction. The direction to this point differed by 5 percent of the maximum possible. The Model 4 direction for the transport was within 1 percent of the forecasted value using the Model 3 forecast, but only within 8 percent of the value obtained with this forecast using Model 4. This points up the fact that was made earlier concerning the Model 3 diffusion prediction being less sensitive than a Model 4 diffusion prediction to the forecasted meteorological condition.

TABLE 5. MODEL 3 SURFACE EXHAUST CLOUD LENGTH AND TRANSIT TIME PREDICTIONS

Range from Launch Complex (m)	Exhaust Cloud Length on Surface (m)	Arrival Time (sec)	Passage Time (sec)
1793	0	149	149
2293	125	182	191
2793	250	214	233
3293	375	247	274
3793	500	279	316
4293	624	311	358
4793	749	344	399
5293	874	376	441
5793	999	409	483
6293	1124	441	524
7293	1374	506	608
8293	1624	571	691
9293	1873	636	775
10293	2123	701	858
12793	2748	863	1066
15293	3372	1025	1275
17793	3997	1187	1483
20293	4621	1349	1692

TABLE ι. PREDICTIONS FOR INSTRUMENT SITES AT LAUNCH TIME UTILIZING MODEL 4

Station Range (km)	CC 1.44	EE 0.99	DD 0.76	BB 0.70
Peak Concentration				
HCl (ppm)	2.1×10^{-4}	1.7	0.79	3.3×10^{-10}
CO (ppm)	3.7×10^{-4}	3.0	1.4	5.8×10^{-10}
CO_2 (ppm)	2.4×10^{-5}	0.20	0.09	3.8×10^{-11}
Al_2O_3 (mg/m^3)	4.7×10^{-4}	3.8	1.8	7.4×10^{-10}
Peak Dosage				
HCl (ppm sec)	3.6×10^{-3}	25	8.7	2.8×10^{-9}
CO (ppm sec)	6.2×10^{-3}	43	15	4.8×10^{-9}
CO_2 (ppm sec)	4.1×10^{-4}	2.8	1.0	3.2×10^{-10}
Al_2O_3 (mg sec/m^3)	8.0×10^{-3}	55	19	6.2×10^{-10}
Cloud Arrival Time (min)	1.8	1.2	0.87	0.79
Cloud Passage Time (min)	2.5	1.8	1.4	1.3
Cloud Width (m)	958	708	585	554
Cloud Length (m)	480	390	348	337

Note:

Ground Cloud Heading: 46.5 deg
Ground Cloud Transport Speed: 11.3 m/sec

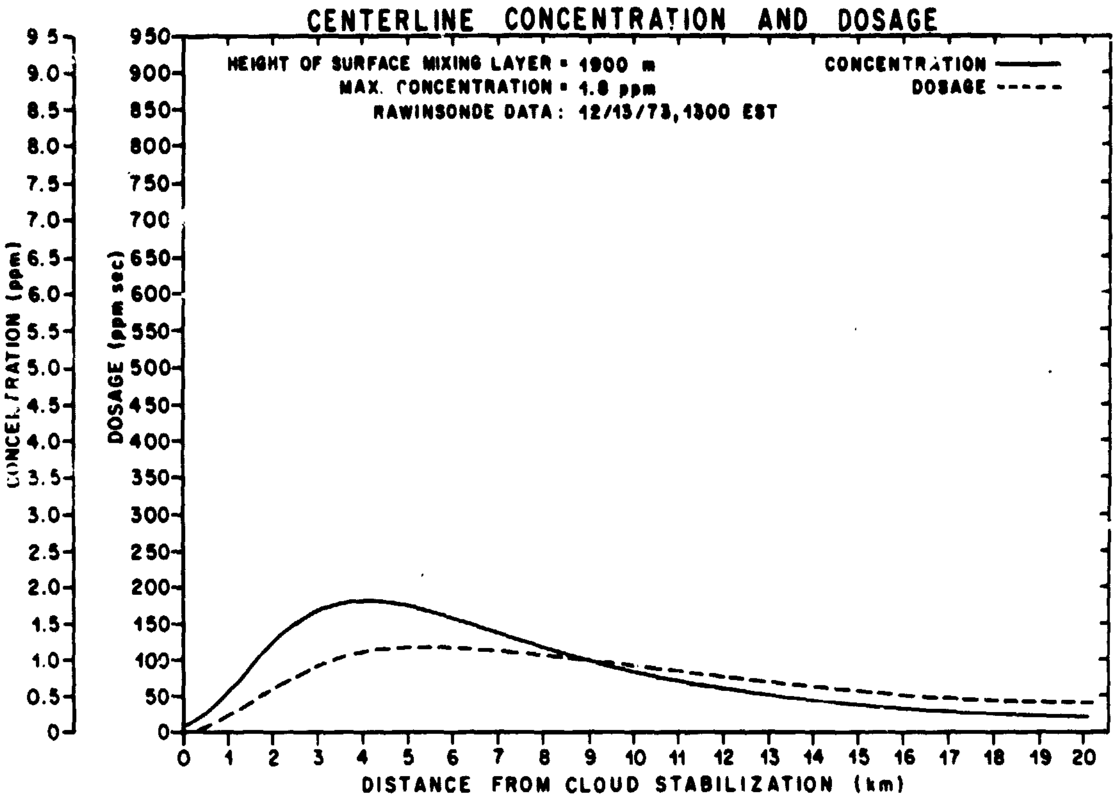

Figure 10. Forecast predictions for the launch centerline concentrations and dosages (T-6 hours).

An examination of parametric sensitivity affords an uncertainty estimate. A parameter which is extremely critical to these diffusion predictions is the surface conditions. Two Model 3 launch predictions were made using the T-0 rawinsonde sounding. In one case the surface conditions at the release point for the rawinsonde sounding (10 km from the launch complex) were used, and in the other case (launch profile used) the surface conditions were taken from Tower 110 about 1 km from the launch complex. The 1 deg lower temperature at the tower resulted in a 29-m difference in cloud stabilization height. This resulted in a 0.6 ppm lower maximum concentration in the prediction using tower surface conditions rather than the surface conditions at the rawinsonde release point. The release point data would have improved the transport directional difference between the forecast and launch prediction by 2 deg. It can be argued, therefore, that there is about a 15-percent uncertainty in the launch prediction based just on the uncertainty of meteorological kinematics

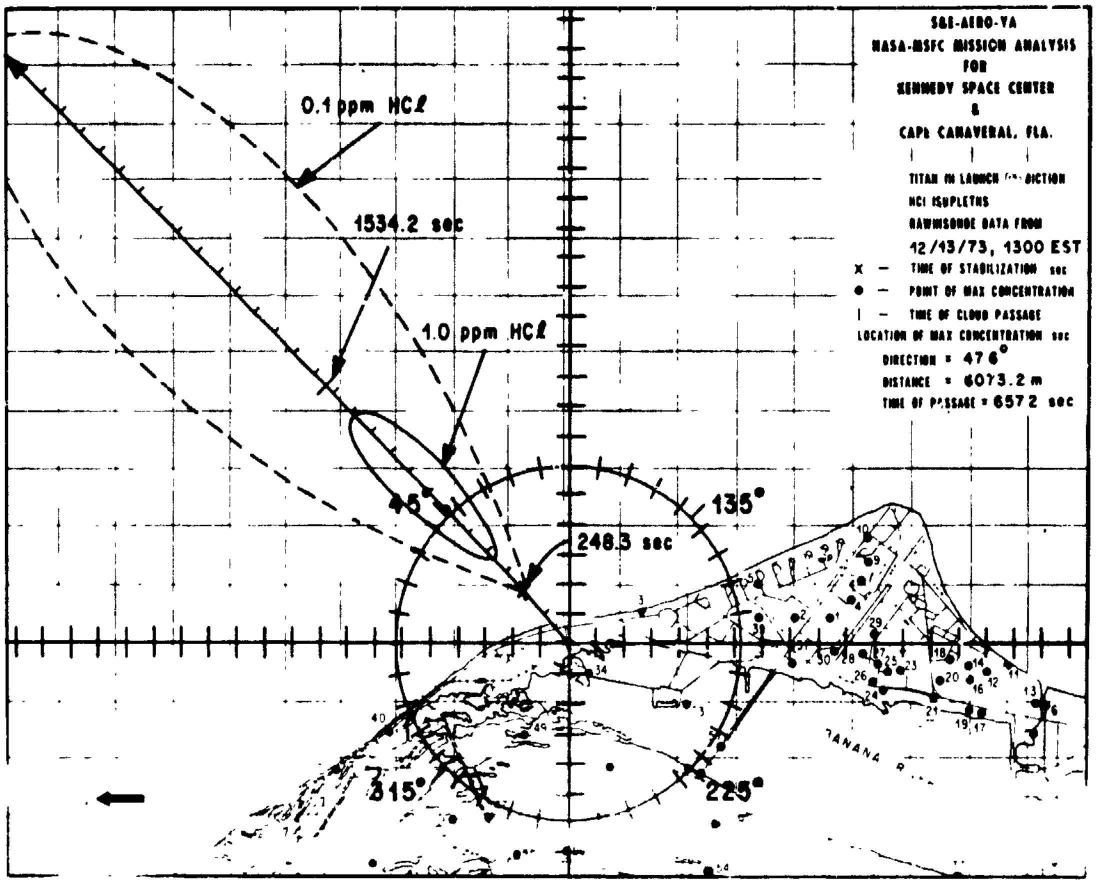

Figure 11. Model 3 forecast predictions for HCl isopleths at launch (T-6 hours).

and thermodynamics. Since our forecasted predictions are within these limits, we feel that they are very good; however, when these predictions are compared with measurements, we do not feel in this special case that they are too good with respect to the cloud stabilization height.

According to the analysis of the Titan exhaust cloud measurements obtained with the Askania tracking units by Dr. R. B. Stewart, Langley Research Center, the ground cloud stabilized at an altitude of about 1500 m (Fig. 12). This is almost a factor of three higher than the predicted stabilization height. This is a strange result in view of the good tradition of Briggs equations in the prediction of other Titan cloud stabilization heights [9]. However, the exhaust cloud's transit path was unique from the other case in that it

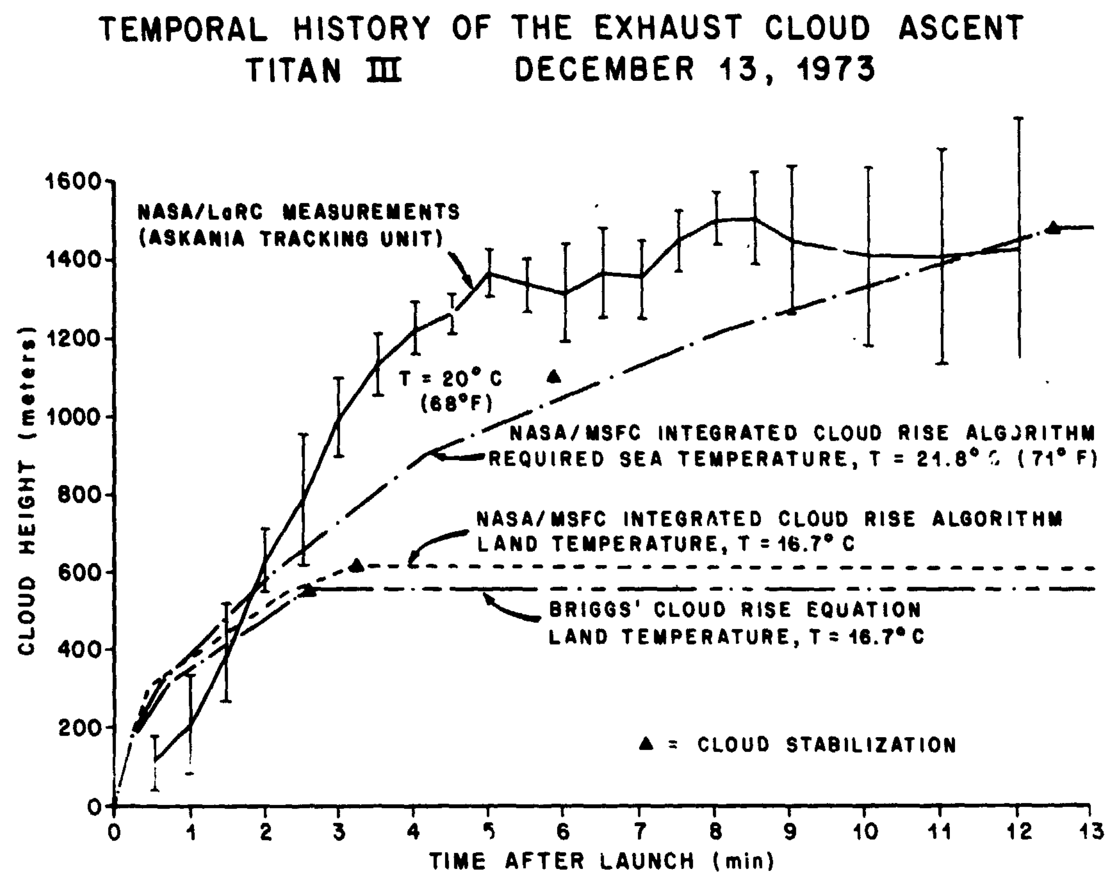

Figure 12. Analysis of the temporal ascent of the Titan IIIC exhaust cloud.

involved a land-sea interface where a large temperature gradient existed because of the right time conditions. A closer examination of the problem showed that the wrong boundary conditions at the surface were probably used — specifically, the ocean temperature should have been used as the surface temperature.

To suppress the sensitivity to small uncertainties in the surface temperature in the Briggs equations and to more fully reflect the thermodynamic profile of the atmosphere, the NASA/MSFC Integrated Cloud Rise algorithms were developed. These algorithms differ from the Briggs equations in that they utilize linear regression analysis to obtain the potential temperature gradient and the surface temperature rather than the two-point value used by

Briggs. Using the NASA/MSFC Integrated Cloud Rise algorithms, the measured exhaust cloud stabilization height corresponds to a surface temperature of 20° C to 22° C, which is roughly the ocean temperature.

The net impact of the underestimation of the cloud stabilization height is to overestimate the strength of the concentration and dosages. From the standpoint of hazards analysis, this kind of estimate is not adverse; however, more precision is desired. Our preliminary conclusions are that the ocean temperature dominates the cloud rise when the cloud's transit path is out to sea. However, more empirical data are required before a definite statement can be made.

SECTION IV. CONCLUSION

J. Briscoe Stephens

The Aerospace Environment Division, Marshall Space Flight Center, made rocket exhaust effluent diffusion predictions for the launch of the Titan IIIC from the Eastern Test Range at Cape Canaveral Air Force Station on December 13, 1973, at 1857 EST. These diffusion predictions were designed to afford Langley Research Center a forecast for the dispersive transport of the Titan exhaust effluents for the deployment of their monitoring instrumentation as well as an opportunity to develop confidence limits for the NASA/MSFC Multilayer Diffusion Predictions. The forecasted diffusion predictions for the instrument deployment 6 hours prior to the launch were extremely close to the actual launch diffusion predictions in view of the intricate meteorological forecast requirements for these predictions.

Real-time diffusion predictions were made based on a forecast for the atmospheric launch conditions starting about 23 hours before the launch. These early predictions were made to identify the general area of the effluent transport as a guide to the preliminary planning for instrument deployment. The diffusion forecast 6 hours prior to launch was the one that Langley Research Center utilized for the actual deployment of their instrumentation and is, thus, the forecast of primary importance to the measurements program. For this reason we limited the diffusion results which were presented here to the T-6 hour forecast and the T-0 launch predictions.

The maximum concentration of hydrogen chloride was predicted — utilizing the launch rawinsonde sounding — to be 2.0 ppm according to the spherical diffusion model (Model 3). This is a factor of two less than the 10-min public limit; therefore, we can conclude that there was not an adverse ecological consequence from this Titan launch. Our 6-hour forecast predicted a maximum concentration of hydrogen chloride of 1.8 ppm, and this forecast predicted slightly fatter isopleths.

The greatest difference between the forecasted diffusion parameters and the launch diffusion parameters was in the range from the launch complex to the point of maximum concentration — there was a 15-percent difference due largely to our failure to forecast the surface temperature inversion. The difference between the forecast and launch transit directions was 5 percent of the maximum possible difference, which is more than a factor of two better than the 11-percent uncertainty we feel is normally associated with this forecast.

A comparison of diffusion results using different surface conditions that were measured in the area at launch time suggests that the uncertainty in these parameters would introduce a little less than a 15-percent uncertainty into our diffusion results. Since our forecasted values compared with the launch values by less than the uncertainty in the meteorology conditions, we can only conclude that the forecast was extremely good. To obtain a less conservative exhaust cloud stabilization height, we found that it is probably necessary to use the ocean temperature rather than the land temperature for the surface temperature in the cloud rise calculations when the exhaust cloud is transported out to sea.

APPENDIX A

EXHAUST EFFLUENT CLOUD RISE ALGORITHM FOR THE TITAN

J. Briscoe Stephens

The exhaust effluent cloud's temporal ascent history to the point of the stabilization height is dependent on the atmospheric thermodynamic profile and the effective heat released by the rocket motor. The thermodynamic characteristics of the atmosphere are reflected by the potential temperature (Φ). The potential temperature is effectively a normalization of the dry bulb temperature (T) with pressure (p:mb) such that

$$\Phi_z = T_z \left(\frac{1000}{p_z}\right) \quad \frac{R}{c_p} = 0.288 \quad , \tag{A-1}$$

which is to say that this is the temperature that a mass of dry air would attain if it were brought from its initial state at an altitude equal to a pressure of 1000 mb by an isentropic state change (i.e., adiabatically). In terms of an energy balance, the vertical entropy gradient ($\partial s/\partial z$) can be expressed as

$$\frac{\partial s}{\partial z} = \frac{c_p}{\Phi} \frac{\partial \Phi}{\partial z} \quad , \tag{A-2}$$

where c_p (0.24 cal/g °K) is the specific heat of air. Thus the potential temperature gradient is a measure of the change in energy of the atmosphere. If

$$\frac{\partial \Phi}{\partial z} \leq 0 \quad , \tag{A-3}$$

the atmosphere is unstable; that is, superadiabatic (when equal to zero, it is adiabatic). The exhaust cloud will continue to rise in the unstable atmosphere until a stable atmospheric condition is reached where

$$\frac{\partial \Phi}{\partial z} > 0 \quad . \tag{A-4}$$

The temporal ascent of the exhaust cloud from a Titan is described by an instantaneous exhaust effluent cloud rise algorithm (spherical entrainment) due to the short residence time of this vehicle on the pad.

The general form for the temporal exhaust cloud effluent ascent history in an unstable atmosphere is given by [8]

$$z = \left[\frac{2Ft^2}{\gamma^3\bar{u}^2} + \left(\frac{r_R}{\gamma}\right)^4\right]^{1/4} - \frac{r_R}{\gamma} \quad , \qquad \text{(A-5)}$$

where the buoyancy parameter (F) is

$$F = \left(\frac{3gQ}{4\pi\rho_s c_p T_s}\right) \qquad \text{(A-6)}$$

and the stability parameter (s) is

$$s = \frac{g}{T_s} \left.\frac{\Delta\Phi}{\Delta z}\right|_{z\text{-surface}} \quad . \qquad \text{(A-7)}$$

The symbols denoting the surface temperature and density of the ambient air are T_s and ρ_s. The symbol used for the mean air speed in the surface mixing layer is $\bar{u}$, the heat release of the Titan is Q, the entrainment coefficient is γ (0.64), the time after ignition is t, and the gravitational acceleration is g (9.8 m/se r_R is the initial cloud radius, which is taken as zero for the Titan [4]. Thus, the temporal cloud rise history for the Titan under adiabatic or superadiabatic conditions is given by

$$z = \left[\frac{2Ft^2}{\gamma^3\bar{u}^2}\right]^{1/4} \quad . \qquad \text{(A-8)}$$

The general form for the temporal ascent of the exhaust effluent cloud in a stable atmosphere is [8]

$$z = \left\{ \frac{4F_m}{\gamma^3 s^{1/2}} \sin(s^{1/2} t) + \frac{4F}{\gamma^3 s} [1 - \cos(s^{1/2} t)] + \left[\frac{r_R}{\gamma}\right]^4 \right\}^{1/4} - \frac{r_R}{\gamma} \quad , \tag{A-9}$$

where F_m is the initial momentum parameter. The maximum cloud rise occurs when $t = \pi/s^{1/2}$, which allows us to express the height of cloud stabilization (H) as

$$H = \left\{ \frac{8F}{\gamma^3 s} + \left(\frac{r_R}{\gamma}\right)^4 \right\}^{1/4} - \frac{r_R}{\gamma} \quad . \tag{A-10}$$

Utilizing the constraints for the Titan where F_m is negligible when compared with F and r_e is approximately zero, the temporal ascent history of the exhaust cloud is [from equation (A-9)]

$$z \doteq \left\{ \frac{4F}{\gamma^3 s} [1 - \cos(s^{1/2} t)] \right\}^{1/4} \quad . \tag{A-11}$$

It should be noted that for an unstable lapse rate s is negative, which results in an imaginary argument for the cosine and an imaginary time of cloud stabilization (t_s),

$$t_s = \frac{\pi}{s^{1/2}} \quad . \tag{A-12}$$

This is why these algorithms afford a suitable description only for the stable lapse rate.

The height of the exhaust cloud stabilization for the Titan is [from equation (A-10)]

$$H = \left[\frac{8F}{\gamma^3 s}\right]^{1/4} \quad , \tag{A-13}$$

where F and s are functions of the stabilization height. Based on information supplied by A. E. Weller of Battelle Columbus Laboratories and H. E. Cramer Company [4], the effective heat release (Q: cal) is

$$Q = 1.609907 \times 10^{9} H^{0.4837} \tag{A-14}$$

for the Titan. Thus, the exhaust effluent cloud rise algorithms do not have a closed form. This transcendental equation requires an iterative solution that is performed by selecting an altitude and calculating the potential temperature gradient and the heat release. These values are in terms substituted into the cloud rise algorithm to determine if the selected altitude is a solution.

APPENDIX B

THE DESCRIPTION OF THE NASA/MSFC MULTILAYER DIFFUSION MODEL AND THE NASA/MSFC SURFACE-LAYER DIFFUSION PROGRAM

J. Briscoe Stephens

The functions of the six different models which constitute the NASA/MSFC Multilayer Diffusion Model [2] are summarized here. Since the description of the dispersion for a volume source is of primary concern in the diffusion predictions of the Titan III exhaust effluents, the algorithms associated with this Model 3 description are given. Finally, the algorithms employed in the diffusion description for the NASA/MSFC Surface-Layer Diffusion Program are discussed [1].

A. The Description of the Models in the NASA/MSFC Multilayer Diffusion Model

The normal launch environment, which has an impact on the transport of exhaust effluents, will usually involve an atmospheric structure comprised of several horizontal meteorological layers with distinctive wind velocity and temperature regimes between the surface and a 2-km altitude. Large horizontal spatial variation in these meteorological parameters may also occur in the surface layer as a consequence of changes in terrain or land-water interfaces, which also must be accounted for by the diffusion model. The general diffusion model does not account for these variations, since it assumes a uniform expanding volume about a moving point of reference in a homogeneous environment.

To overcome the obvious shortcomings of the general diffusion model but to stay within the established bounds of classical fluid mechanics [3], a multiple layer concept is introduced to cope with the vertical and horizontal atmospheric thermodynamic and kinematic gradients. Here, the general diffusion model is applied to individual horizontal layers in which the meteorological structure is reasonably homogeneous and independent of the neighboring layers. These layers have boundaries which are placed points of major discontinuities in the vertical profiles of wind velocity and temperature. Since the Multilayer Diffusion Model has imposed the general restriction of layer independence (no flux of particles or gases entering or leaving an individual layer), special provision must be made for spatial changes in the horizontal meteorology if known and for gravitational settling or precipitation scavenging. In addition, the type of source within a layer must be considered; that is, whether there is a ground cloud source or a plume cloud source (see Symbols and Definitions).

The NASA/MSFC Multilayer Diffusion Model has six models (Fig. B-1) which account for three categories of dispersive constraints: the source distribution, the environmental effects, and the depositional effects. This flexibility is required to deal with the stages of the development of the exhaust cloud and the complex, potentially varying meteorological conditions. These models can be used alone to describe all the environmental layers or in superimposed combinations where variations in layer meteorology require different modeling. For the introductory overview, however, these combinations will not be considered. The primary objective of the output of all these models is a spatial delineation of the concentrations and dosages of the individual exhaust constituents. The one-dimensional delineation gives the centerline profile of the level of concentrations and dosages along the exhaust cloud's transit path, whereas the two-dimensional delineation gives the mapping of the concentrations and dosage isopleths (contours of constant levels).

The fundamental category of dispersive constraints is the source distribution. The two distributions are:

1. The elliptic-cylindrical source which assumes a two-dimensional Gaussian distribution in the x-y plane and a uniform distribution in the vertical direction.

2. The ellipsoidal source which assumes a three-dimensional Gaussian distribution.

Model 1 is for the elliptic-cylindrical source whose vertical expansion is constrained by the layer boundaries — and thus has only a two-dimensional expansion in the horizontal plane due to turbulence mixing. This model is normally used to describe the rocket's inflight plume cloud.

Model 3 is for the ellipsoidal source and is assumed to expand in all three dimensions as the effluents are propagated downstream. When the ellipsoidal source reaches the top of the mixing layer, the distribution of the constituents is reflected back into the expanding vertical distribution. On the other hand, that fraction not lost in surface deposition is also reflected back in a similar manner. After sufficient mixing, the ellipsoidal distribution becomes an elliptic-cylindrical distribution (Model 1). While Model 3 is normally used

Toxic Solid Rocket Exhaust Product	Time Interval (min)	Concentration		
		Public	Emergency	Occupational[b]
Alumina (Al_2O_3)	10	5.0 mg/m^3	x	50 mg/m^3
	30	2.5 mg/m^3	x	25 mg/m^3
	60	1.5 mg/m^3	x	15 mg/m^3
	480	1.0 mg/m^3	x	10 mg/m^3
Hydrogen Chloride (HCl)	10	4 ppm	7 ppm	30 ppm
	30	2 ppm	3 ppm	20 ppm
	60	2 ppm	3 ppm	10 ppm
Carbon Monoxide (CO)	10	90 ppm	275 ppm	1000 (1500)[c] ppm
	30	35 ppm	100 ppm	500 (800)[c] ppm
	60	25 ppm	66 ppm	200 (400)[c] ppm
Dosage:		200 ppm/ time interval		
Carbon Dioxide (CO_2)	480	x	x	Average: 5000 ppm
		x	x	Peak: 6250 ppm

NOTE:
Parts of vapor or gas per million parts of contaminated air by volume at 25°C and 760 mm Hg.

a. These values were reviewed on the phone by Ralph C. Wands, Director, Advisory Center on Toxicology, National Academy of Sciences, 2101 Constitution Avenue, Washington, D. C. 20418, April 1973.

b. EPA suggests that a safety factor of ten be applied to occupational exposure limits.

c. At these concentrations, headaches will occur along with a loss in work efficiency.

Figure B-1. Block diagram of the computer program for the NASA/MSFC Multilayer Diffusion Model.

to describe the dispersion of the rocket's ground cloud, it could be used to model upper air explosions. The formulation for Model 3 has been provided in Appendix B and will be employed in this analysis of the transport of the Titan III exhaust effluents.

The second category is environmental effects. The two effects are:

1. No turbulence mixing in the upper atmosphere.

2. Changes in meteorological conditions as a function of altitude and as the constituents are transported downstream.

Model 2 is the same as Model 1 except it is assumed that there is no turbulent mixing. This implies that the exhaust material just meanders along the layer without dispersing. While Model 2 is not generally used, movies of rocket firings clearly show that under some special meteorological conditions this model is required. While the Multilayer Diffusion Model is general in applicability, it is specific in meteorological parameters and launch description.

Model 4 is primarily utilized to ensure the proper distribution of the material in the exhaust cloud and an initial division of the atmosphere into thermodynamically and kinematically homogeneous layers. If the information concerning the atmospheric variations along the exhaust cloud's transit path are known (in general, there is only a single rawinsonde sounding available for the region of interest), these variations can be introduced into the diffusion description afforded by this model. This model assumes that the vertical concentration of material is uniform throughout each layer, dispersing only in the horizontal plane until layer breakdown (usually occurs about 1 sec after stabilization). When layer breakdown occurs, the boundaries are removed and each layer is treated as a separate volume source (Model 3) which is superimposed on the other sources to give the resulting concentration and dosage fields in accordance with the new layers.

The third category of dispersive constraints includes the deposition due to:

1. Precipitation scavenging.

2. Gravitational settling.

Model 5 accounts for precipitation scavenging. An example of where Model 5 must be used is in solid rocket launches during the occurrence of rain because the HCl will be scavenged by the rain. Model 6 describes the ground deposition due to gravitational settling of particles or droplets. Wind shears are incorporated in this model to account for the effect of the settling velocity of the particulate matter. There are two forms for the source in this model:

1. The source that extends vertically through the entire layer with a uniform distribtuion — this is the same source model as used with Models 1 and 2.

2. A volume source in the Kth layer — this is the same source model as used with Model 3 or Model 4 depending on the modeling technique desired.

Our interest in this discussion of the Titan III launch will be restricted to Models 3 and 4 of the NASA/MSFC Multilayer Diffusion Model. Model 3 tends to be more than adequate when a meteorological forecast is being utilized as an input for modeling the atmospheric diffusion, since there is a certain amount of uncertainty associated with the forecasted atmospheric parameters which tends to be averaged out over the surface mixing layer. Model 4, on the other hand, only averages over a layer (initially, there are about six layers normally in the surface mixing layer) and, therefore, Model 4 is more sensitive to the kinematic profile of the atmosphere. In general then, Model 4 is more suited to diffusion predictions where a rawinsonde sounding is available.

B. Concentration-Dosage Formulation for NASA/MSFC Multilayer Diffusion Model [2]

The fundamental relation for the concentration-dosage calculation is presented for the ellipsoidal source used in Model 3. These relations are appropriate to the elliptic-cylindrical distribution of Model 1 if the vertical dispersive interaction is neglected. This part of the appendix is complex and is, therefore, only recommended when a detailed scientific knowledge is required.

The dosage equation for Model 3 in the Kth layer is given by the expression [2]

$$
\begin{aligned}
D_K\{x_K, y_K, z_{BK} < z_K < z_{TK}\} = \frac{Q_K}{2\pi\, \sigma_{yK}\, \sigma_{zK}\, u_K} & \left\{ \exp\left[\frac{-y_K^2}{2\sigma_{yK}^2}\right]\right\}\left\{\exp\left[\frac{-(H_K - z_K)^2}{2\sigma_{zK}^2}\right]\right. \\
& + \exp\left[\frac{-(H_K - 2z_{BK} + z_K)^2}{2\sigma_{zK}^2}\right] \\
& + \sum_{i=1}^{\infty} \left\{ \exp\left[\frac{-\left(2i(z_{TK} - z_{BK}) - (H_K - 2z_{BK} + z_K)\right)^2}{2\sigma_{zK}^2}\right]\right. \\
& + \exp\left[\frac{-\left(2i(z_{TK} - z_{BK}) + (H_K - z_K)\right)^2}{2\sigma_{zK}^2}\right] \\
& + \exp\left[\frac{-\left(2i(z_{TK} - z_{BK}) - (H_K - z_K)\right)^2}{2\sigma_{zK}^2}\right] \\
& \left.\left. + \exp\left[\frac{-\left(2i(z_{TK} - z_{BK}) + (H_K - 2z_{BK} + z_K)\right)^2}{2\sigma_{zK}^2}\right]\right\}\right\} \quad . \qquad \text{(B-1)}
\end{aligned}
$$

where Q_K corresponds to the source strength or total mass of material in the layer and H_K is the height of the centroid of the stabilized cloud.

The standard deviation of the vertical dosage distribution (σ_{zK}) is defined by the expression

$$
\sigma_{zK} = \sigma'_{EK}\, x_{rzK} \left(\frac{x_K + x_{zK} - x_{rzK}(1 - \beta_K)}{\beta_K\, x_{rzK}} \right)^{\beta_K} \quad , \qquad \text{(B-2)}
$$

where σ'_{EK} describes the mean standard deviation of the wind elevation angle, x_{zK} gives the vertical virtual distance, β_K accounts for vertical diffusion, and x_{rzK} is the distance over which rectilinear vertical expansion occurs downwind from an ideal point source in the Kth layer.

In the surface layer $(K = 1)$, the standard deviation of the wind elevation angle (σ_{ER}) at the height z_R is described by

$$\sigma_{EK}\{K = 1\} = \frac{\sigma_{ER}\left[(z_{TK}\{K = 1\})^{q+1} - (z_R)^{q+1}\right]}{(q + 1)(z_{TK}\{K = 1\} - z_R)(z_R)^q} \left(\frac{\pi}{180}\right) \quad , \quad \text{(B-3)}$$

where the power-law exponent (q) for the vertical profile of the standard deviation of the wind elevation angle in the surface layer is

$$q = \log\left(\frac{\sigma_{ETK}\{K = 1\}}{\sigma_{ER}}\right) \Big/ \log\left(\frac{z_{TK}\{K = 1\}}{z_R}\right) \quad ; \quad \text{(B-4)}$$

here $\sigma_{ETK}\{K = 1\}$ is the standard deviation of the wind elevatio angle at the top of the surface layer. Above the surface layer $(K > 1)$, the standard deviation of the wind elevation angle is

$$\sigma'_{EK}\{K > 1\} = (\sigma_{ETK} + \sigma_{EBK}) \left(\frac{\pi}{360}\right) \quad , \quad \text{(B-5)}$$

where σ_{EBK} are the standard deviations of the wind elevation angle at the top and at the base of the layer.

The vertical virtual distance x_{zK} is given by the expression

$$\left\{\begin{array}{ll} \dfrac{\sigma_{zo}\{K\}}{\sigma'_{EK}} - x_{RzK} & ; \ \sigma_{zo}\{K\} \le \sigma'_{EK}\, x_{rzK} \\[2ex] \beta_K\, x_{rzK}\left(\dfrac{\sigma_{zo}\{K\}}{\sigma'_{EK}\, x_{rzK}}\right)^{1/\beta_K} - x_{RzK} + x_{rzK}(1 - \beta_K) & ; \ \sigma_{zo}\{K\} \ge \sigma'_{EK}\, x_{rzK} \end{array}\right\} , \quad \text{(B-6)}$$

where $\sigma_{zo}\{K\}$ is the standard deviation of the vertical dosage distribution at x_{RzK}, the distance from the source where the measurement is made in the Kth layer.

The remaining terms are common also to Model 1; that is, what has just been discussed is to account for the vertical expansion of the source cloud.

The quantity $\bar{u}_K$ in equation (B-1) is the mean cloud transport speed in the Kth layer. In the surface layer $(K = 1)$, the wind speed-height profile is defined according to the power-law expression

$$\bar{u}\{z_K, K = 1\} = \bar{u}_R \left(\frac{z_K\{K = 1\}}{z_R}\right)^p \quad , \tag{B-7}$$

where $\bar{u}_R$ is the mean wind speed measured at the reference height z_R, and the power-law exponent (p) for the wind speed profile in the surface layer is described by

$$p = \log\left(\frac{\bar{u}_{TK}\{K = 1\}}{\bar{u}_R}\right) \Bigg/ \log\left(\frac{z_{TK}\{K = 1\}}{z_R}\right) \quad ; \tag{B-8}$$

here $\bar{u}_{TK}\{K = 1\}$ corresponds to the mean wind speed at the top of the surface layer $(z_{TK}\{K = 1\})$. Thus, in the surface layer, the mean cloud transport speed $(u\{K = 1\})$ is

$$\bar{u}_K\{K = 1\} = \frac{\bar{u}_R}{(z_{TK}\{K = 1\} - z_R)\, z_R^{\,p}} \int_{z_R}^{z_{TK}} (z_K\{K = 1\})^p \, dz \quad , \tag{B-9}$$

which reduces to

$$\bar{u}_K\{K = 1\} = \frac{\bar{u}_R\left[(z_{TK}\{K = 1\})^{1+p} - (z_R)^{1+p}\right]}{(z_{TK}\{K = 1\} - z_R)(z_R)^p\,(1 + p)} \quad . \qquad \text{(B-10)}$$

In layers above the surface layer $(K > 1)$, the wind speed-height profile $(\bar{u}\{z_K, K > 1\})$ is assumed linear and defined as

$$\bar{u}\{z_K, K > 1\} = \bar{u}_{BK} + \left(\frac{\bar{u}_{TK} - \bar{u}_{BK}}{z_{TK} - z_{BK}}\right)(z_K - z_{BK}) \quad , \qquad \text{(B-11)}$$

where $\bar{u}_{TK}$ and $\bar{u}_{BK}$ describe the mean wind speed at the top of the layer and at the base of the layer, respectively. In the Kth layer $(K > 1)$, the mean cloud transport speed $(\bar{u}_K\{K > 1\})$ is

$$\bar{u}_K\{K > 1\} = (\bar{u}_{TK} + \bar{u}_{BK})/2 \quad . \qquad \text{(B-12)}$$

The standard deviation of the crosswind dosage distribution (σ_{yK}) is defined by

$$\sigma_{yK} = \left\{\left[\sigma'_{AK}\{\tau_K\}\, x_{ryK}\left(\frac{x_K + x_{yK} - x_{ryK}(1 - \alpha_K)}{\alpha_K\, x_{ryK}}\right)^{\alpha_K}\right]^2 + \left[\frac{\Delta\theta'_K\, x_K}{4.3}\right]^2\right\}^{1/2} \quad , \qquad \text{(B-13)}$$

where $\sigma'_{AK}\{\tau_K\}$ corresponds to the mean layer standard deviation of the wind azimuth for the cloud stabilization time (τ_K). In the surface layer $(K = 1)$,

$$\sigma'_{AK}\{\tau_K, K = 1\} = \frac{\sigma'_{AR}\{\tau_K\} \left[(z_{TK}\{K = 1\})^{m+1} - (z_R)^{m+1} \right]}{(m + 1)(z_{TK}\{K = 1\} - z_R)(z_R)^m} \quad , \tag{B-14}$$

where the standard deviation of the wind azimuth angle $(\sigma'_{AR}\{\tau_K\})$ at height z_R and for the cloud stabilization time τ_K is

$$\sigma'_{AR}\{\tau_K\} = \sigma_{AR}\{\tau_{oK}\} \left(\frac{\tau_K}{\tau_{oK}} \right)^{1/5} \cdot \left(\frac{\pi}{180} \right) \quad ; \tag{B-15}$$

here $\sigma_{AR}\{\tau_{oK}\}$ is the standard deviation of the wind azimuth angle at height z_R and for the reference time period (τ_{oK}), and the power-law exponent (m) for the vertical profile of the standard deviation of the wind azimuth angle in the surface layer is

$$m = \log \left(\frac{\sigma'_{ATK}\{\tau_K, K = 1\}}{\sigma'_{AR}\{\tau_K\}} \right) \Big/ \log \left(\frac{z_{TK}\{K = 1\}}{z_R} \right) \quad . \tag{B-16}$$

Then,

$$\sigma'_{ATK}\{\tau_K, K = 1\} = \sigma_{ATK}\{\tau_{oK}, K = 1\} \left(\frac{\tau_K}{\tau_{oK}} \right)^{1/5} \left(\frac{\pi}{180} \right) \quad , \tag{B-17}$$

where $\sigma_{ATK}\{\tau_{oK}, K = 1\}$ is the standard deviation of the wind azimuth angle at the top of the surface layer for the reference time period. For layers above the surface $(K > 1)$,

$$\sigma'_{ATK}\{\tau_K, K > 1\} = \left(\sigma'_{ATK}\{\tau_K\} + \sigma'_{ABK}\{\tau_K\}\right)\Big/2 \quad , \qquad \text{(B-18)}$$

where

$$\sigma'_{ATK}\{\tau_K\} = \sigma_{ATK}\{\tau_{oK}\}\left(\frac{\tau_K}{\tau_{oK}}\right)^{1/5}\left(\frac{\pi}{180}\right) \quad ; \qquad \text{(B-19)}$$

here $\sigma_{ATK}\{\tau_K\}$ is the standard deviation of the wind azimuth angle at the top of the layer.

$$\sigma'_{ABK}\{\tau_K\} = \sigma_{ABK}\{\tau_{oK}\}\left(\frac{\tau_K}{\tau_{oK}}\right)^{1/5}\left(\frac{\pi}{180}\right) \quad ; \qquad \text{(B-20)}$$

here $\sigma_{ABK}\{\tau_{oK}\}$ is the standard deviation of the wind azimuth angle in degrees at the base of the layer for the reference time period (τ_{oK}).

The crosswind virtual distance is

$$x_{yK} = \frac{\sigma_{yo}\{K\}}{\sigma'_{AK}\{\tau_K\}} - x_{RyK} \qquad \text{(B-21)}$$

when

$$\sigma_{yo}\{K\} \leq \sigma'_{AK}\{\tau_K\}\, x_{ryK} \quad ,$$

or

$$x_{yK} = \alpha_K\, x_{ryK} \left(\frac{\sigma_{yo}\{K\}}{\sigma'_{AK}\{\tau_K\}\, x_{ryK}} \right)^{1/\alpha_K} - x_{RyK} + x_{ryK}(1 - \alpha_K) \qquad \text{(B-22)}$$

when

$$\sigma_{yo}\{K\} \geq \sigma'_{AK}\{\tau_K\}\, x_{ryK} \quad ;$$

here $\sigma_{yo}\{K\}$ is the standard deviation of the lateral source dimension in the layer at downwind distance x_{RyK}, x_{ryK} is the distance over which rectilinear crosswind expansion occurs downwind from an ideal point source, and α_K describes the lateral diffusion in the layer. The vertical wind direction shear $(\Delta\theta'_K)$ is the layer is

$$\Delta\theta'_K = (\theta_{TK} - \theta_{BK}) \left(\frac{\pi}{180}\right) \quad , \qquad \text{(B-23)}$$

where θ_{TK} and θ_{BK} are the mean wind direction at the top and at the base of the layer, respectively.

The concentration algorithm is of the same form for the first three models; however, the dosage term (D_K) does depend on which model has been utilized and thus adjusts the concentration description to the specific model of interest.

The maximum concentration for the first three models in the Kth layer is given by the expression

$$\chi_K\{x_K, y_K, z_K\} = \frac{D_K\, \bar{u}_K}{\sqrt{2\pi}\, \sigma_{xK}} \quad , \qquad \text{(B-24)}$$

where the standard deviation of the along-wind concentration distribution (σ_{xK}) in the layer is

$$\sigma_{xK} = \left[\left(\frac{L\{x_K\}}{4.3}\right)^2 + \sigma_{xo}^2\{K\}\right]^{1/2} , \qquad \text{(B-25)}$$

and the along-wind cloud length ($L\{x_K\}$) for a point source in the layer at the distance x_K from the source is

$$L\{x_K\} = \left\{\begin{array}{ll} \dfrac{0.28\,(\Delta\bar{u}_K)(x_K)}{\bar{u}_K} & ; \ \Delta\bar{u}_K \geq 0 \\ 0 & ; \ \Delta\bar{u}_K \leq 0 \end{array}\right\} , \qquad \text{(B-26)}$$

where $\Delta\bar{u}_K$ is the vertical wind speed shear in the layer and is defined as

$$\Delta\bar{u}_K\{K = 1\} = \bar{u}_{TK}\{K = 1\} - \bar{u}_R \qquad \text{(B-27)}$$

or

$$\Delta\bar{u}_K\{K > 1\} = \bar{u}_{TK} - \bar{u}_{BK} \qquad \text{(B-28)}$$

and $\sigma_{xo}\{K\}$ is the standard deviation of the along-wind source dimension in the layer at the point of cloud stabilization. The above equation for $L\{x_K\}$ is based on the theoretical and empirical results reported by Tyldesley and Wallington [10] who analyzed ground-level concentration measurements made at distances of 5 to 120 km downwind from instantaneous line-source releases.

The maximum centerline concentration for the model in the Kth layer is given by the expression

$$\chi_{CK}\{x_K, y_K = 0, z_K\} = \chi_K / \{\text{LATERAL TERM}\} \quad . \tag{B-29}$$

The average along-wind concentration is defined as

$$\bar{\chi}_K = D_K / t_{pK} \quad , \tag{B-30}$$

where the ground cloud passage time in seconds is

$$t_{pK} \cong 4.3\, \sigma_{xK} / \bar{u}_K \quad . \tag{B-31}$$

The time mean along-wind concentration in the Kth layer is defined by the expression

$$\chi_K\{x_K, y_K, z_K; T_A\} = \frac{D_K}{T_A} \left\{ \text{erf} \left(\frac{\bar{u}_K T_A}{2\sqrt{2}\, \sigma_{xK}} \right) \right\} \quad , \tag{B-32}$$

where T_A is the time in seconds over which concentration is to be averaged. The time mean along-wind concentration is equivalent to the average along-wind concentration when t_{pK} equals T_A. This complex set of relations, then, contains the computations performed in Model 3 to obtain the concentration-dosage mappings.

C. Titan III Version of NASA/MSFC Diffusion Model [1]

By specialization of the NASA/MSFC Multilayer Diffusion Model for Titan III exhaust effluents, the prediction for the ground level concentration isopleths are obtained from a small programmable desk calculator (HP 9820) in real time. The modeling approach employed is as follows.

The meteorological profile is utilized in layering the atmosphere in accordance with homogeneous kinematic and thermodynamic properties — hence the name "Multilayer Diffusion Model." The specialization of the general NASA/MSFC Multilayer Diffusion Model has limited the layers of consideration to just the surface mixing layer. In addition, we assume that the source has an elliptical shape with ellipsoidal expansion (Model 3 of the NASA/MSFC Multilayer Diffusion Model).

Thus, the dosage algorithm is

$$
\begin{aligned}
D\{x, y, z_B < z < z_T\} = \frac{Q}{2\pi\,\sigma_y \sigma_z \bar{\bar{u}}} & \left\{ \exp\left[\frac{-y^2}{2\sigma_y^{\,2}}\right]\right\} \left\{ \exp\left[\frac{-(H-z)^2}{2\sigma_z^{\,2}}\right] \right. \\
& + \exp\left[\frac{-(H - 2z_B + z)^2}{2\sigma_z^{\,2}}\right] \\
& + \sum_{i=1}^{\infty} \left\{ \exp\left[\frac{-\left(2i(z_T - z_B) - (H - 2z_B + z)\right)^2}{2\sigma_z^{\,2}}\right] \right. \\
& + \exp\left[\frac{-\left(2i(z_T - z_B) + (H - z)\right)^2}{2\sigma_z^{\,2}}\right] \\
& + \exp\left[\frac{-\left(2i(z_T - z_B) - (H - z)\right)^2}{2\sigma_z^{\,2}}\right] \\
& \left. \left. + \exp\left[\frac{-\left(2i(z_T - z_B) + (H - 2z_B + z)\right)^2}{2\sigma_z^{\,2}}\right] \right\} \right\} , \quad \text{(B-33)}
\end{aligned}
$$

where Q corresponds to the source strength or total mass of material in the surface mixing layer, H is the height of the centroid of the stabilized cloud, and the subscripts T and B stand for the top and bottom.

By restricting the dosage mapping to the surface and defining the bottom of the layer as the surface, equation (B-33) simplifies to

$$D\{x, y, 0\} = \frac{Q}{2\pi\,\sigma_y \sigma_z\,\bar{u}} \left\{ \exp\left[\frac{-y^2}{2\sigma_y^2}\right]\right\} \left\{ 2 \exp\left[\frac{-H}{\sigma_z^2}\right] + \sum_{i=1}^{n} \left\{ 2 \exp\left[\frac{-(2i\, z_T + H)^2}{\sigma_z^2}\right] + 2 \exp\left[\frac{-(2i\, z_T + H)^2}{\sigma_z^2}\right]\right\}\right\} , \qquad \text{(B-34)}$$

where z_T is the altitude of the top of the surface mixing layer and n is such that the first exponential in the summation is no greater than 225. This is the specialized dosage algorithm that we use.

The standard deviations of the vertical distribution (σ_z) and the crosswind distribution (σ_y) are defined as follows:

1. The standard deviation of the vertical dosage distribution is defined by the expression

$$\sigma_z = \sigma'_E\, x_{rz} \left[\frac{x + x_z - x_{rz}(1 - \beta)}{\beta\, x_{rz}}\right]^{\beta} , \qquad \text{(B-35)}$$

where σ'_E describes the mean standard deviation of the wind elevation angle, x_z gives the vertical virtual distance, β accounts for vertical diffusion, and x_{rz} is the distance over which rectilinear vertical expansion occurs downwind from an ideal point source.

In this specialization, we assume that the vertical diffusion coefficient is one $(\beta = 1)$ which permits us to rewrite equation (B-35) as

$$\sigma_z = \sigma'_E (x + x_z) \quad . \tag{B-36}$$

In the surface layer, the standard deviation of the wind elevation angle (σ_{ER}) at the height z_R is described by

$$\sigma'_E = \frac{\sigma_{ER}\left[(z_{T'})^{q+1} - (z_R)^{q+1}\right]}{(q+1)(z_T - z_R)(z_R)^q} \left(\frac{\pi}{180}\right) \quad , \tag{B-37}$$

where the power-law exponent (q) for the vertical profile of the standard deviation of the wind elevation angle in the surface layer is

$$q = \log\left(\frac{\sigma_{ET}}{\sigma_{ER}}\right) \Bigg/ \log\left(\frac{z_T}{z_R}\right) \quad , \tag{B-38}$$

where σ_{ET} is the standard deviation of the wind elevation angle at the top of the surface layer.

The vertical virtual distance x_z is given by the expression

$$x_z = \frac{\sigma_{zo}}{\sigma'_E} - x_{Rz} \quad , \tag{B-39}$$

where σ_{zo} is the standard deviation of the vertical dosage distribution at x_{Rz}, the distance from the source where the measurement is made in the surface mixing layer.

2. The standard deviation of the crosswind dosage distribution is defined by

$$\sigma_y = \left\{ \left[\sigma'_A\{\tau\}\, x_{ry} \left(\frac{x + x_y - x_{ry}(1-\alpha)}{\alpha\, x_{ry}} \right)^{\alpha} \right]^2 + \left(\frac{\Delta\theta'\, x}{4.3} \right)^2 \right\}^{1/2} \quad , \tag{B-40}$$

where $\sigma'_A\{\tau\}$ corresponds to the mean layer standard deviation of the wind azimuth for the cloud stabilization time (τ). The difference in wind direction $(\Delta\theta'$: radians) is taken between the surface and the top of the surface mixing layer in accordance with

$$\Delta\theta' = (\theta_T - \theta_B) \left(\frac{\pi}{180} \right) \quad , \tag{B-41}$$

where θ_T and θ_B are the mean wind direction at the top and at the base of the layer, respectively. This is the wind shear. If we again assume that the diffusion coefficient is one $(\alpha = 1)$, then equation (B-39) becomes

$$\sigma_y = \left\{ \left[\sigma'_A\{\tau\}\ (x + x_y) \right]^2 + \left(\frac{\Delta\theta'\, x}{4.3} \right)^2 \right\}^{1/2} \quad . \tag{B-42}$$

From the relation we can observe how important a factor the wind shear is in determining the crosswind distribution of the effluent. In the surface layer

$$\sigma'_A\{\tau_K\} = \frac{\sigma'_{AR}\{\tau\} \left[(z_T)^{m+1} - (z_R)^{m+1} \right]}{(m+1)(z_T - z_R)(z_R)^m} \quad , \tag{B-43}$$

where the standard deviation of the wind azimuth angle $(\sigma'_{AR}\{\tau\})$ at height z_R and for the cloud stabilization time τ is

$$\sigma'_{AR}\{\tau\} = \sigma_{AR}\{\tau_o\} \left(\frac{\tau}{\tau_o}\right)^{1/5} \left(\frac{\pi}{180}\right) \quad , \tag{B-44}$$

where $\sigma_{AR}\{\tau_o\}$ is the standard deviation of the wind azimuth angle at height z_R and for the reference time period (τ_o), and the powe_-law exponent (m) for the vertical profile of the standard deviation of the wind azimuth angle in the surfr ce layer is

$$m = \log\left(\frac{\sigma'_{AT}\{\tau\}}{\sigma'_{AR}\{\tau\}}\right) \Big/ \log\left(\frac{z_T}{z_R}\right) \quad . \tag{B-45}$$

Then

$$\sigma'_{AT}\{\tau\} = \sigma_{AT}\{\tau_o\} \left(\frac{\tau}{\tau_o}\right)^{1/5} \left(\frac{\pi}{180}\right) \quad , \tag{B-46}$$

where $\sigma_{AT}\{\tau_o\}$ is the standard deviation of the wind azimuth angle at the top of the surface layer for the reference time period.

The crosswind virtual distance is

$$x_y = \frac{\sigma_{yo}}{\sigma'_A\{\tau\}} - x_{Ry} \quad , \tag{B-47}$$

where σ_{yo} is the standard deviation of the lateral source dimension at downwind distance x_{RY}, and x_{ry} is the distance over which rectilinear crosswind expansion occurs downwind from an ideal point source.

3. The mean speed of cloud transport $(\bar{u})$ in the surface layer is defined in accordance with the power law

$$\bar{u}\{z\} = \bar{u}_R \left(\frac{z}{z_R}\right)^p \quad , \tag{B-48}$$

where $\bar{u}_R$ is the mean wind speed measured at the reference height z_R, and the power-law exponent (p) for the wind speed profile in the surface layer is described by

$$p = \log\left(\frac{\bar{u}_T}{\bar{u}_R}\right) \Bigg/ \log\left(\frac{z_T}{z_R}\right) \quad , \tag{B-49}$$

where $\bar{u}_T$ corresponds to the mean wind speed at the top of the surface layer (z_T). Thus, in the surface layer, the mean cloud transport speed $(\bar{u})$ is

$$\bar{u} = \frac{\bar{u}_R}{(z_T - z_R)\, z_R^{\ p}} \int_{z_R}^{z_T} z^p \, dz \quad , \tag{B-50}$$

which reduces to

$$\bar{u} = \frac{\bar{u}_R \left[(z_T)^{1+p} - (z_R)^{1+p}\right]}{(z_T - z_R)(z_R)^p (1 + p)} \quad . \tag{B-51}$$

The concentration (χ) follows directly from the results for the dosage (D) algorithm given by equation (B-33). The average concentration then is just

$$\chi\{x,y,z\} = D\{x,y,z\} \left(\frac{\bar{u}}{4.3\,\sigma_x}\right) \quad , \tag{B-52}$$

where the standard deviation of the along-wind concentration distribution (σ_x) in the layer is

$$\sigma_x = \left[\left(\frac{L\{x\}}{4.3}\right)^2 + \sigma_{xo}^{\ 2}\right]^{1/2} \quad , \tag{B-53}$$

and the along-wind cloud length $(L\{x\})$ for a point source in the layer at the distance x from the source is

$$L\{x\} = \frac{0.28\,(\Delta\bar{u})(x)}{\bar{u}} \qquad \Delta\bar{u} \geq 0$$

$$\qquad = 0 \qquad \Delta\bar{u} \leq 0 \quad . \tag{B-54}$$

Here $\Delta\bar{u}$ is the vertical wind speed shear in the layer and is defined as

$$\Delta\bar{u} = \bar{u}_T - \bar{u}_R \quad , \tag{B-55}$$

and σ_{xo} is the standard deviation of the along-wind source dimension in the layer at the point of cloud stabilization. The above equation for $L\{x\}$ is based on the theoretical and empirical results reported by Tyldesley and Wallington [10] who analyzed ground-level concentration measurements made at distances of 5 to 120 km downwind from instantaneous line-source releases.

In summary, it should be pointed out that the standard deviation of the vertical, crosswind, and along-wind terms represents the cloud dimensions (L_i); that is

$$L_i = 4.3\,\sigma_i \quad . \tag{B-56}$$

The factor 4.3 represents the 97-percent confidence level of a normal distribution. Hence, the initial source dimension is translated into the standard deviation initially for modeling. The standard deviations σ_x, σ_y, σ_z give the cloud size during the diffusion process.

APPENDIX C

INPUT PARAMETERS FOR THE NASA/MSFC MULTILAYER DIFFUSION MODEL

J. Briscoe Stephens

There are two groups of input parameters for the model. The source input parameters which are vehicle and meteorologically dependent (Table C-1) and the meteorological input parameters which are strictly dependent on meteorological conditions at launch time (Table C-2). These parameters include the special set employed in the layer breakdown model (Model 4).

The source relationships given in Table C-1 are determined in reference to the stabilized ground cloud. The standard deviation of the crosswind source is

$$\sigma_{yo}\{K\} = \frac{Y\{K\}}{4.3} , \tag{C-1}$$

and the standard deviation of the along-wind source is

$$\sigma_{xo}\{K\} = \frac{X\{K\}}{4.3} . \tag{C-2}$$

The source strength in the Kth layer is

$$Q_K = \frac{Y\{K\}\ X\{K\}}{\Sigma\, Y\{K\}\ x\{K\}} \quad \frac{Q_T}{z_{TK} - z_{BK}} , \tag{C-3}$$

where $Y\{K\}$ and $X\{K\}$ describe the crosswind and along-wind dimensions of the cloud in the Kth layer and Q_T is the total source strength in the ground cloud in units of mass.

TABLE C-1. SOURCE INPUTS FOR THE MULTILAYER MODEL CALCULATIONS

Parameter		
Layer Model 1, 2, 3	Layer Breakdown Model 4	Definition
z_R	z_R	Reference height in the surface layer
z_{BK}	z_{BL}	Height of the layer base
z_{TK}		Height of the layer top
τ_K	τ_L	Source (cloud) stabilization time
x_{ryK}	x_{ryL}	Distance over which rectilinear lateral expansion occurs downwind from an ideal point source
$\sigma_{yo}\{K\}$		Standard deviation of the crosswind source dimension in the Kth layer
$\sigma_{xo}\{K\}$		Standard deviation of the along-wind source dimension in the Kth layer
	t*	Time of layer breakdown
Q_K		Source strength in the layer
J		Scaling coefficient

Equations (C-1) and (C-2) are based on the assumption that the along-wind and crosswind distribution of material in each layer is Gaussian and that the visible edge of the cloud represents the point at which the concentration is one-tenth the concentration at the cloud center in the Kth layer. Equation (C-3) assumes that the cloud is spheroidal in the plane of the horizon and that the total source strength in the Kth layer is given by the relative cloud volume in the Kth layer. Because the models require the source strength per unit height, the total source strength in the Kth layer must be divided by the depth of the layer.

TABLE C-2. LIST OF METEOROLOGICAL MODEL INPUTS

Parameter		
Layer Model 1, 2, 3	Layer Breakdown Model 4	Definition
$\bar{u}_R$	$\bar{u}_{RL}$	Mean wind speed at reference height z_R
$\bar{u}_{BK}$	$\bar{u}_{BL}$	Mean wind speed at the base of the layer
$\bar{u}_{TK}$	$\bar{u}_{TL}$	Mean wind speed at the top of the layer
θ_{BK}	θ_{BL}	Mean wind direction at the base of the layer
θ_{TK}	θ_{TL}	Mean wind direction at the top of the layer
$\sigma_{AR}\{\tau_{oK}\}$	$\sigma_{ARL}\{\tau_{oL}\}$	Standard deviation of the wind azimuth angle at height z_R
$\sigma_{ABK}\{\tau_{oK}\}$	$\sigma_{ABL}\{\tau_{oL}\}$	Standard deviation of the wind azimuth angle at the base of the layer
$\sigma_{ATK}\{\tau_{oK}\}$	$\sigma_{ATL}\{\tau_{oL}\}$	Standard deviation of the wind azimuth angle at the top of the layer
τ_{oK}	τ_{oL}	Reference time period
α_K	α_L	Lateral diffusion coefficient
$p\{K = 1\}$	$p\{L = 1\}$	Power-law exponent of the wind speed profile in the surface layer
	σ_{ERL}	Standard deviation of the wind elevation angle at height z_R
	σ_{EBL}	Standard deviation of the wind elevation angle at the base of the Lth layer

TABLE C-2. (Concluded)

Parameter		
Layer Model 1, 2, 3	Layer Breakdown Model 4	Definition
	σ_{ETL}	Standard deviation of the wind elevation angle at the top of the Lth layer
	β_L	Vertical diffusion coefficient

The first nine meteorologic parameters follow directly from the thermodynamic and kinematic profiles of the atmosphere. The remaining two parameters (layer model) are empirical atmospheric constants.

APPENDIX D

TOXICITY CRITERIA

J. Briscoe Stephens, John W. Kaufman, Leonard L. DeVries
Michael Susko, and C. Kelly Hill

Realistic evaluation of the potential hazard arising from high near-field concentrations of toxic effluents from solid rocket exhausts requires both a knowledge of the surface deposition of these effluents, which can be obtained with the MSFC/NASA Multilayer Diffusion Model (Appendix B), and toxicity criteria to evaluate the hazard from this surface deposition of effluent, which is the purpose of this discussion. The Federal Air Quality Criteria do not presently include any of the liquid or solid rocket exhaust effluents; however, the National Academy of Sciences does afford definite guidelines for the exposure to the toxic effluents associated with these exhausts. These guidelines are ecologically sound, based on the current limited knowledge of the effects of these effluents, and are the basis of the toxicity criteria that will be given [11, 12].

The primary effluents from any solid rocket exhaust are aluminum oxide (Al_2O_3), hydrogen chloride (HCl), carbon monoxide (CO), carbon dioxide (CO_2), hydrogen (H_2), nitrogen (N_2), and water vapor (H_2O). While only the first four compounds are toxic in significant concentrations, there is always a potential hazard of suffocation from any gas which results in the reduction of the partial pressure of oxygen to a level below 135 mm Hg (18 percent by volume at STP). Oxygen level reduction does not appear to be a hazard from rocket exhausts because of the large volume of air that is entrained into these exhaust clouds; therefore, this potential hazard can be neglected in this discussion and attention can be directed to only the initial four toxic compounds. (A liquid rocket motor has only one toxic effluent, carbon monoxide.)

The exposure level for toxic effluents is divided into three categories: public exposure level, emergency public exposure level, and occupational exposure level. The public exposure levels are designed to prevent any detrimental health effects both to all classes of human beings (children, men, women, the elderly, those of poor health, etc.) and to all forms of biological life. The emergency level is designed as a limit in which some detrimental effects may occur, especially to biological life. The occupational level gives the maximum allowable concentration that a man in good health can tolerate; this level could be hazardous to various forms of biological life.

The toxicity criteria for the toxic effluents in solid rocket exhausts are given in Table D-1. Public health levels for aluminum oxide are not given because the experience with these particulates is so limited that, at best, the industrial limits are just good estimates.

Hydrogen chloride is an irritant; therefore, the concentration criterion for an interval should not be exceeded [12]. Since hydrogen chloride is detrimental to biological life, and in view of the fact that most launch sites are encompassed by wild life refuges, the emergency and industrial criteria for hydrogen chloride are not appropriate to the ecological constraints. Because of the large volume of air entrained in the exhaust cloud, the potential hazard from carbon monoxide and carbon dioxide can be, in general, neglected.

Any detrimental health effects resulting from combined toxicological action of these ingredients have been omitted because of a lack of knowledge in this area. However, investigations are currently underway to study this problem and to learn more about the biological effects of hydrogen chloride.

TABLE D-1. AIR QUALITY TOXICITY STANDARDS[a]

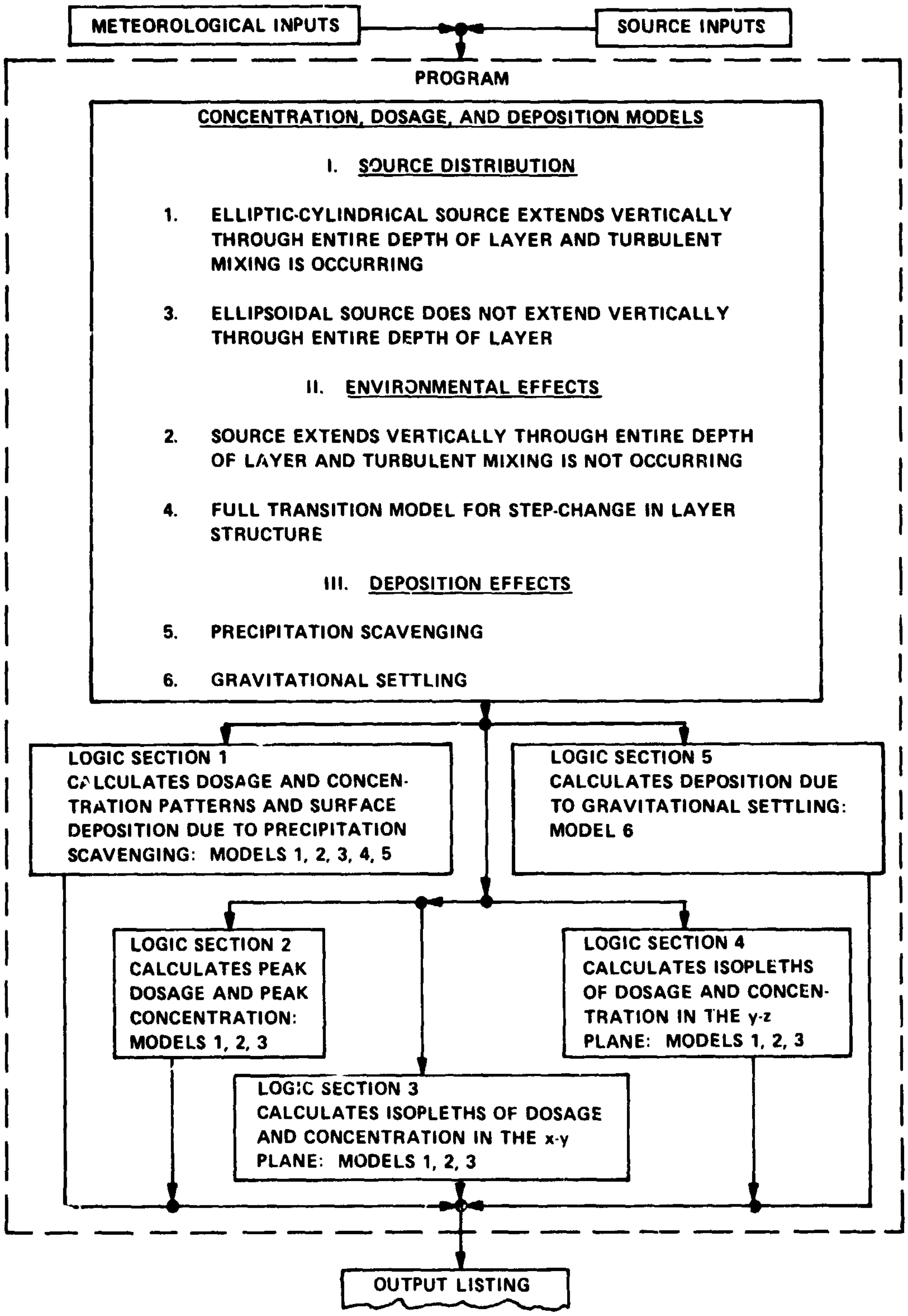

REFERENCES

1. Stephens, J. Briscoe; and Hamilton, Philip A.: Diffusion Algorithms and Data Reduction Routine for On-Site Launch Predictions for the Transport of Titan IIIC Exhaust Effluents. NASA TN D-7862, December 1974.
2. Dumbauld, R. K.; Bjorklund, J. R.; and Bowers, J. F.: NASA/MSFC Multilayer Diffusion Models and Computer Program for Operational Prediction of Toxic Fuel Hazards. NASA CR-129006, June 1973.
3. Slale, David H., ed: Meteorology and Atomic Energy, 1968. TID-24190, NBS, U.S. Department of Commerce, Springfield, Va., July 1968.
4. Dumbauld, R. K.; Cramer, H. E.; Bowers, J. F.; and Bjorklund, J. R.: Downwind Hazard Calculations for Titan IIIC Launches at Kennedy Space Center and Vandenberg Air Force Base. Report under Contract No. NAS8-29033, H. E. Cramer Co., TR-73-301-04, November 1973.
5. Stephens, J. Briscoe; Susko, Michael; Kaufman, John W.; and Hill, C. Kelly: An Analytical Analysis of the Dispersion Predictions for Effluents from the Saturn V and Scout-Algol III Rocket Exhausts. NASA TM X-2935, October 1973.
6. Susko, Michael; Kaufman, John W.; and Hill, C. Kelly: Rise Rate and Growth of Static Test Vehicle Engine Exhaust Clouds. NASA TM X-53782, October 15, 1968, pp. 146-166.
7. Thayer, Scott D.; Chandler, Martin W.; and Chu, Roland T.: Rise and Growth of Space Vehicle Engine Exhaust and Associated Diffusion Models. NASA CR-61331, July 1970.
8. Briggs, G. A.: Some Recent Analyses of Plume Rise Observations. Paper presented at the 1970 International Union of Air Pollution Prevention Associations, Atmospheric Turbulence and Diffusion Laboratory, National Oceanic and Atmospheric Administration, Oak Ridge, Tennessee, USA, ATDL, No. 38, 1970.
9. Cramer, H. E.; Dumbauld, R. K.; Geary, H. V.; and Bjorklund, J. R.: Analysis of meteorological and exhaust cloud data from SAMTEC Operation 2707. H. E. Cramer Co., Tech. Rpt. TR-4-001-01 under Contract DAAD09-71-C-0003 with Deseret Test Center, DTC Project No. DTC-TR-72-610 with Space and Missile Test Center, Vandenberg AFB, Calif, 1972.

REFERENCES (Concluded)

10. Tyldesley, J. B.; and Wallington, C. E.: The Effect of Wind Shear and Vertical Diffusion on Horizontal Dispersion. Quart. J. Roy. Met. Soc., vol. 91, 1967, pp. 158-174.

11. National Primary and Secondary Ambient Air Quality Standards. Environmental Protection Agency, Part II of Federal Register, vol. 36, no. 84, April 1971 (Updated November 1971).

12. Guides for Short-Term Exposures of the Public to Air Pollutants, Volume II, Guide for Hydrogen Chloride. Committee on Toxicology of the National Academy of Sciences, National Research Council, Washington, D. C., August 1971.

APPROVAL

ATMOSPHERIC DIFFUSION PREDICTIONS FOR THE EXHAUST EFFLUENTS FROM THE LAUNCH OF A TITAN IIIC, DECEMBER 13, 1973

J. Briscoe Stephens, Editor

The information in this report has been reviewed for security classification. Review of any information concerning Department of Defense or Atomic Energy Commission programs has been made by the MSFC Security Classification Officer. This report, in its entirety, has been determined to be unclassified.

This document has also been reviewed and approved for technical accuracy.

GEORGE H. FICHTL
Chief, Environmental Dynamics Branch

WILLIAM W. VAUGHAN
Chief, Aerospace Environment Division

CHARLES A. LUNDQUIST
Director, Space Sciences Laboratory

☆U.S. GOVERMENT PRINTING OFFICE 1975–640-454/305 REGION NO 4